THE DEVELOPMENT OF AN OPTICALLY ACTIVE LASER SCHLIEREN SYSTEM WITH APPLICATION TO HIGH PRESSURE SOLID PROPELLANT COMBUSTION

James Randolph Andrews

NAVAL POSTGRADUATE SCHOOL
Monterey, California

THESIS

THE DEVELOPMENT OF AN OPTICALLY ACTIVE LASER SCHLIEREN SYSTEM WITH APPLICATION TO HIGH PRESSURE SOLID PROPELLANT COMBUSTION

by

James Randolph Andrews

September 1975

Thesis Advisor: D.W. Netzer

REPORT DOCUMENTATION PAGE

READ INSTRUCTIONS BEFORE COMPLETING FORM

1. REPORT NUMBER	2. GOVT ACCESSION NO. / 3. RECIPIENT'S CATALOG NUMBER
4. TITLE (and Subtitle): The Development of an Optically Active Laser Schlieren System with Application to High Pressure Solid Propellant Combustion	5. TYPE OF REPORT & PERIOD COVERED: Engineer's Thesis; September 1975
	6. PERFORMING ORG. REPORT NUMBER
7. AUTHOR(s): James Randolph Andrews	8. CONTRACT OR GRANT NUMBER(s): ORD 331-007/551-1-332-303
9. PERFORMING ORGANIZATION NAME AND ADDRESS: Naval Postgraduate School, Monterey, California 93940	10. PROGRAM ELEMENT, PROJECT, TASK AREA & WORK UNIT NUMBERS
11. CONTROLLING OFFICE NAME AND ADDRESS: Naval Ordnance Systems Command, Washington, D.C.	12. REPORT DATE: September 1975
	13. NUMBER OF PAGES: 77
14. MONITORING AGENCY NAME & ADDRESS (if different from Controlling Office)	15. SECURITY CLASS. (of this report): Unclassified
	15a. DECLASSIFICATION/DOWNGRADING SCHEDULE

16. DISTRIBUTION STATEMENT (of this Report)

Approved for public release; distribution unlimited.

17. DISTRIBUTION STATEMENT (of the abstract entered in Block 20, if different from Report)

18. SUPPLEMENTARY NOTES

19. KEY WORDS (Continue on reverse side if necessary and identify by block number)

Optically active laser schlieren
Flow visualization-combustion

20. ABSTRACT (Continue on reverse side if necessary and identify by block number)

A laser schlieren system, using an optically active single-piece quartz prism-polaroid sheet combination aperture in place of the conventional knife edge, was developed and applied to high pressure solid propellant combustion studies. Advantages and limitations of the system are discussed. Ammonium perchlorate deflagration was observed to pressures of 2500 psi. Distinct surface reaction sites were evidenced in the gas phase

(20. ABSTRACT Continued)

at high and low pressures by alternating density gradients across the surface. These sites were found to be very small or nonexistent at intermediate pressures.

The Development of an Optically Active Laser Schlieren System with Application to High Pressure Solid Propellant Combustion

by

James Randolph Andrews
Lieutenant Commander, United States Navy
B.S.E.S., Naval Postgraduate School, 1970
M.S.A.E., Naval Postgraduate School, 1974

Submitted in partial fulfillment of the requirements for the degree of

AERONAUTICAL ENGINEER

from the

NAVAL POSTGRADUATE SCHOOL
September 1975

ABSTRACT

A laser schlieren system, using an optically active single-piece quartz prism-polaroid sheet combination aperture in place of the conventional knife edge, was developed and applied to high pressure solid propellant combustion studies. Advantages and limitations of the system are discussed. Ammonium perchlorate deflagration was observed to pressures of 2500 psi. Distinct surface reaction sites were evidenced in the gas phase at high and low pressures by alternating density gradients across the surface. These sites were found to be very small or nonexistent at intermediate pressures.

TABLE OF CONTENTS

I. INTRODUCTION ---------- 12

A. HISTORICAL PERSPECTIVE ---------- 12

B. SOLID PROPELLANT COMBUSTION MODELING --------- 12

C. OPTICAL METHODS IN SOLID PROPELLANT COMBUSTION RESEARCH ---------- 19

II. EXPERIMENTAL APPARATUS AND PROCEDURES ---------- 28

A. APPARATUS AND THEORY OF OPERATION ---------- 28

B. EXPERIMENTAL PROCEDURES AND PROBLEMS --------- 44

1. Introduction ---------- 44

2. Initial System Setup ---------- 45

3. Schlieren Sensitivity Matching ---------- 49

4. Specimen Preparation and Mounting -------- 60

III. RESULTS AND DISCUSSION OF RESULTS ---------- 62

IV. CONCLUSIONS ---------- 73

LIST OF REFERENCES ---------- 75

INITIAL DISTRIBUTION LIST ---------- 78

LIST OF TABLES

I. Specific Rotation of Quartz ---------- 29

LIST OF FIGURES

1. Deflagration Rate of Ammonium Perchlorate in N_2 ---- 15
2. Schematic for AP-Binder Sandwich ---------- 17
3. Multiple Flame Structure Model for AP Composites --- 18
4. Combustion Zones for Double Base Propellants ------- 20
5. Typical Temperature Profiles for Double Base Propellants ---------- 20
6. Specific Rotation of Optically Active Quartz ------- 30
7. Geometric Relationships in the Aperture Prism ------ 33
8. Qualitative Ray Trace Through A Dual Prism System -- 33
9. Photographs of the General Schlieren System -------- 34
10. Diagram of the Complete Schlieren System ---------- 35
11. Real Image Setup ---------- 38
12. Virtual Image Setup ---------- 38
13. Thin Lens Model ---------- 39
14. Photographs of Combustion Bombs ---------- 41
15. Photograph of Mounted Specimen ---------- 43
16. Divergence of Laser Beam ---------- 48
17. Refraction of Light Through Test Section ---------- 50
18. Polaroid-Reference Ray Polarity Orientation -------- 52
19. Density Gradients for Nitrogen ---------- 55
20. Cyclic Intensity Variation with Monotonic Density Gradient ---------- 56
21. Reference Required Total Sensitivity ---------- 57
22. Diffusion Flames ---------- 63
23. AP/PBAA Self-Luminous Elimination ---------- 66
24. Selected Frames of AP Deflagration ---------- 67

SYMBOLS AND UNITS

AP	Ammonium Perchlorate
$\mathring{A}$	Angstrom Units
atm	Atmospheres
α	Prism Angle to Optical Axis (Degrees)
β	Dimensionless Empirical Refraction Constant [Ref. 27]
β	Inverse Square of Wavelength (Fig. 6) $\beta = \lambda^{-2} \times 10^{8}$
cw	Continuous Wave
ϵ	Total Refraction in Radians
ξ	Total Sensitivity Parameter (Deg)
ξ_r	Required Total Sensitivity for Reference Rotation (Deg) (Fig. 21)
f_i	Focal Length of Lens L_i (cm)
L	Test Section Length (cm)
m	Magnification of Object Using Thin Lens Model
M	Slope of Log-Log Plot for Double Base Propellants
μ	Microns

λ	Wavelength in Angstrom Units
MW	Molecular Weight (kg/kg-Mole)
n	Index of Refraction
N	Pressure Exponent for AP
p	Pressure (psi)
p_s	Reference Pressure 760mm Hg
ρ	Gas Density (kg/m^3)
ρ_s	Reference Gas Density at 0°C & 760mm Hg
$(\overline{d\rho/dy})$	Average Gas Density Gradient (kg/m^3)/cm
$d\rho/dy$	Density Gradient (kg/m^3)/cm
$\mathcal{R}$	Universal Gas Constant (J/Kg-Mole-K)
R_i	Gas Constant of Species i (J/Kg-K)
r	Burn Rate
S	Object Distance in Thin Lens Model
S'	Image Distance in Thin Lens Model
T	Temperature (°K)
T	Prism Reference Thickness (Fig. 7)

T_1T_2	Product of Temperature Extremes (Fig. 19)
ΔT	Differential Thickness for Refracted Rays (mm)
X	Position of Reference Ray (Fig. 7)
X,X'	Ratios of S/F and S'/F in Thin Lens Model (Fig. 13)
ΔX	Displacement for Refracted Rays (mm) (Fig. 7)
$\Delta\Phi_t$	Total Rotation of Refracted Rays (Deg)
ϕ_s	Specific Rotation (Deg/mm)
Γ	Environmental Parameter (m^3/Kg)
Ψ	Reference Rotation (45 Deg/cm Test length)

ACKNOWLEDGMENTS

The technical counseling provided by Prof. A. K. Oppenheim and Staff, University of California, Berkeley, California and Prof. D. W. Netzer, Prof. D. J. Collins and Prof. S. H. Kalmbach, U. S. Naval Postgraduate School, Monterey, California are gratefully acknowledged. Additionally, I would like to express special appreciation for technical assistance given by Messrs. Pat Hickey, Ted Dunton, Bob Besel and Glenn Middleton also from the Naval Postgraduate School staff. This work was sponsored by Naval Ordnance Systems Command, ORD TASK 331-007/551-1-332-303.

I. INTRODUCTION

A. HISTORICAL PERSPECTIVE

Until the past several years, solid propellant developments were largely empirical processes due to the very limited understanding of propellant combustion mechanisms within the confines of a burning chamber. From the early phases of World War II to the present, solid propellants have continued to gain in importance in rocket propulsion from small ordnance rockets to long-range nuclear delivery vehicles such as Poseidon and Polaris. The design of solid rocket motors, being intimately related to the combustion characteristics of the propellant, was also largely experimental. Studies during the past two decades have been able to identify many propellant parameters and establish limited but useful models for the immensely complex phenomenon of solid propellant combustion. The development of adequate models is an obvious necessity for the more complete understanding of propellant combustion. In order to develop these models, however, carefully planned and controlled experiments are required in order to provide a realistic foundation.

B. SOLID PROPELLANT COMBUSTION MODELING

The combustion of solid composite propellants is a set of highly complex concurrent reactions involving all three

physical states of a heterogeneous mixture. Accurate modeling would require an accounting for such parameters as propellant composition, initial temperature and pressure, particle sizes, binder types, degree of mixing and the curing conditions, burning surface shape, gas kinetics, inhibitor performance, catalysts effect and, perhaps, several others. Changes in one parameter may cause changes in others and would be reflected in the overall combustion behavior. The desired output of a model is the prediction of such things as burning rates, temperature and pressure sensitivity, adiabatic flame temperatures and susceptibility to combustion instabilities. "Prediction capability is largely dependent upon empirical correlation rather than on analytical models which reflect a fundamental understanding of the combustion processes " [Ref. 1]. The physical and chemical processes, in general, are not fully known or understood. Even if they were fully known, accurate analytical models would be so enormously complex as to be mathematically intractable. Thus, simplified models have been developed for several types of propellants for correlation purposes. These models often naively assume one-dimensional heat transfer, oversimplified kinetics and reaction rates and, perhaps, even fail to account for the liquid phase or accumulation of species on the surface. A general description of solid propellant combustion has been given by Boggs, et.al. [Ref. 1]. The details involving energy and mass diffusion in the immediate region

of the combustion zone remain major points of disagreement for many models. One major area of uncertainty in modeling is the gas phase. Models have been proposed for the most common propellants and ingredients such as ammonium perchlorate (AP), ammonium perchlorate-binder sandwiches, double base propellants, catalytic influences on propellants, etc. Numerous reviews have appeared in the literature.

Ammonium perchlorate, being a very important and common oxidizer, had a natural early entry in combustion modeling attempts. One current model is due to Guirao and Williams [Ref. 2]. They proposed a one-dimensional model for ammonium perchlorate deflagration between 20 and 100 atmospheres. An important result of the Guirao-Williams AP combustion model was the recognition of the liquid melt contribution to the overall combustion process. They concluded that "exothermic condensed-phase reactions occurring in a liquid layer at the surface of ammonium perchlorate, coupled with exothermic gas-phase reactions, are responsible for the steady deflagration of the propellant in the pressure range from 20 to 100 atms. 70% of the heat release is found to occur in the liquid layer." [Ref. 2] The authors emphatically concluded that the deflagration was in fact not one-dimensional, but attempted to simplify the model by implicit averaging over the detail surface structures to explain an average temperature field, chemical composition, chemical kinetics, heat flux and regression rate. Detailed surface

structures (bubbling and frothing, ridges, active sites and needles) as reported by Boggs [Ref. 3] were not explainable using the Guirao-Williams model. AP deflagration is known to be strongly influenced by pressure as shown in Fig. 1. At room temperatures, experimental pressure dependence of the AP burning rate obeys the power law:

$$\text{Burn Rate} = (\text{Constant}) \times P^N$$

with N = 0.77 typically between 20 and 50 atmospheres [Ref. 4]. The lower pressure limit for monopropellant AP combustion was found to be approximately 300 psi [Refs. 2, 3 and 4].

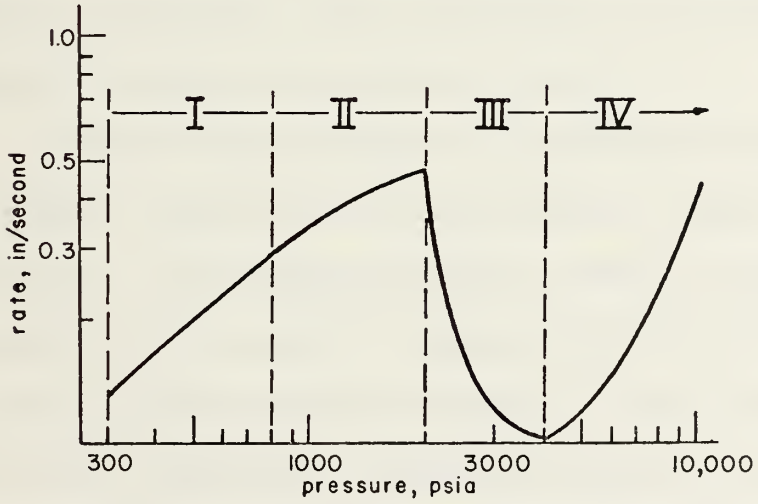

Fig. 1. Deflagration rate of ammonium perchlorate in N_2 (after Boggs, ref. 3)

The sandwich configuration, a layer of binder laminated between two oxidizer layers, is frequently chosen for the

study of the interaction of the ingredients of a composite solid propellant. This allows the rather precise definition of element boundaries immediately prior to reaction. The pseudo two-dimensional sandwich approach represents a compromise between the complexities of the three-dimensional reality of combustion and the oversimplifying assumptions of one-dimensional models. The major benefits of the sandwich approach are that they more readily allow the study of oxidizer-binder interface events and the associated gas phase reactions above the interface. The major objections are a general failure to represent the dimensions of the ingredient layers in actual propellant use, the failure of the reaction zone to encounter a heterogeneity in the direction of burn and the possibility that at some higher experimental pressures, the sandwiches fail to be typical of actual propellant combustion [Ref. 1].

Strahle has provided an analytical model of AP-binder sandwich combustion in the pressure range of 20-100 atm [Ref. 5]. The physical model, shown in Fig. 2, assumes a semi-infinite slab of ammonium perchlorate in contact with a semi-infinite slab of binder. This takes into consideration the regression rates far removed from the interface being pure AP rates, using a slightly modified Guirao-Williams model. Further, this model was time independent (steady state) and free of any catalytic additions or binder melts. It was observed by Strahle that the gas phase binder-oxidizer

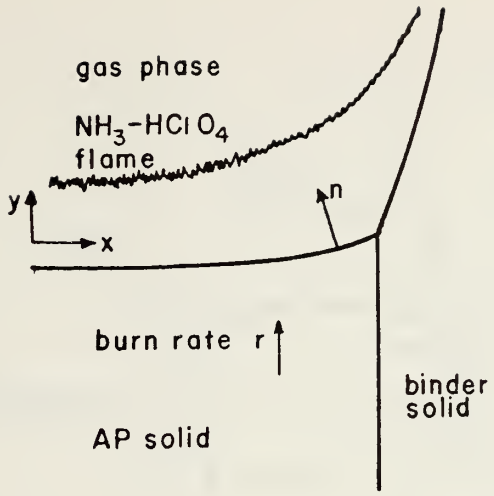

Fig.2 Sandwich schematic
(after Strahle, et al., ref.5)

reactions showed little effect on the surface profile for uncatalyzed sandwiches. This model, therefore, assumed the binder-oxidizer reaction rates to be negligible. Some additional simplifying assumptions were: identical thermal and transport processes of the solid AP and binder, unity Lewis number everywhere in the gas phase, constant pressure deflagration, and identical thermal and transport properties of all gas phase species. A final major assumption was "that on any vertical line parallel to the binder-oxidizer interface the (ρV) product (density times velocity) is that as determined in the solid phase and all lateral velocities are zero" [Ref. 5].

One of the more recent models for ammonium perchlorate composite solid propellants has been proposed by Beckstead, Derr and Price [Ref. 6]. This model was based on the flame structure surrounding individual AP crystals embedded in a binder (Fig. 3). The binder matrix and crystal relationships

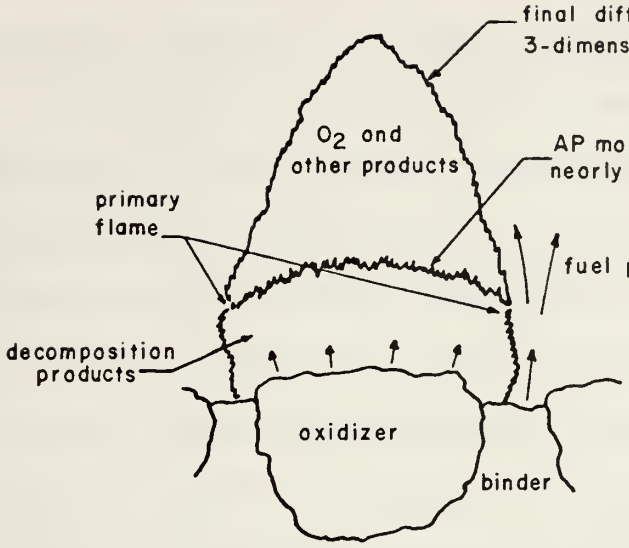

Fig. 3 Multiple flame structure model for AP composites (after Beckstead, et al., ref. 6)

were then statistically evaluated. The intended model objective was not burning rate prediction per se but rather the prediction of a change in burn rate for a given change in propellant composition. Three flame zones were identified: a primary flame between the decomposing binder and the AP, a premixed oxidizer flame and a final diffusion flame between the products of the other two flames. The oxidizer (AP) decomposition was taken to be the dominant factor for the overall combustion process. This model resulted in good agreement with experiment for the effects of surface temperature, pressure exponent, AP concentration and temperature sensitivity on burning rates. The model also assumes an exothermic AP partial decomposition and reaction at the propellant surface in a thin melt region.

For double base propellants, the combustion wave is generally considered to consist of four identifiable regions,

as shown in Figs. 4 and 5. A recent model for double base combustion is due to Kubota, et. al. [Ref. 7]. This model was also one-dimensional with temperature as a predominant parameter. The typical "four-zone" structure was used consisting of the surface reaction layer, the "fizz" zone with the first steep temperature gradient in the gas phase, the "dark" zone with a near constant temperature, and the luminous zone which includes the final combustion processes [Refs. 7 and 8]. Typically, a nitrate ester double base propellant, without catalytic additives, was found to exhibit a near constant pressure exponent function (slope of the log P-log R plot) as follows:

$$M = D(\text{Log}(\text{Rate}))/D(\text{Log}(\text{Pressure}))$$

M was typically between 0.7 and 0.8. This pressure dependence function is known as Vieille's Law. The burning rate of double base propellant is thought to be governed by the reactions and kinetics occurring in the thin surface reaction and fizz zones. Current models for double base propellants, including the effect of catalytic addition, are reported by Kubota, et. al. [Ref. 8].

C. OPTICAL METHODS IN SOLID PROPELLANT COMBUSTION RESEARCH

Numerous optical techniques have been devised to gain insight into the dominant mechanisms in solid propellant deflagration. For example, high speed motion pictures,

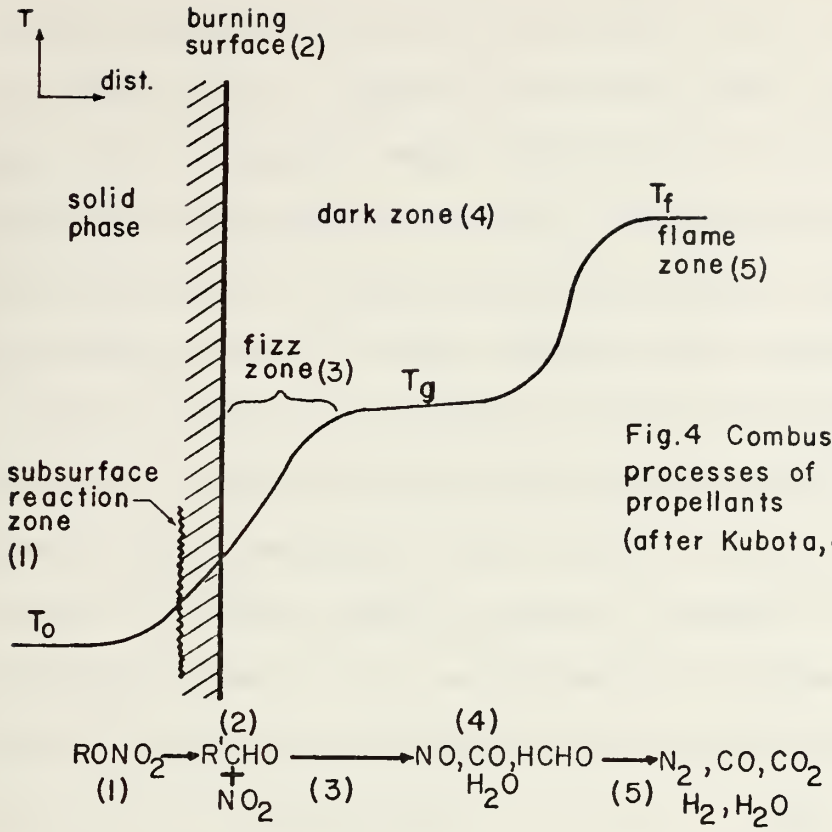

Fig.4 Combustion zones and processes of double base propellants (after Kubota, et al., ref. 7)

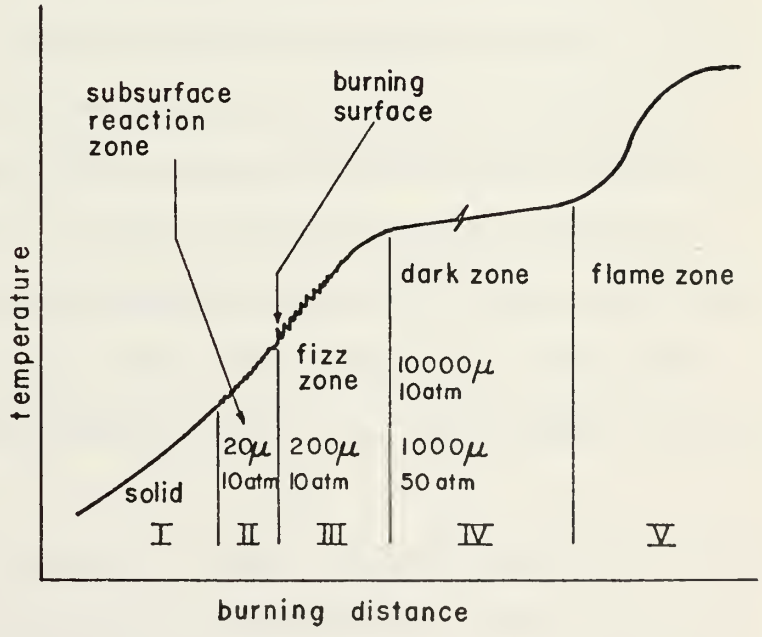

Fig.5 Typical temperature profile for double base propellants (after Kubota, et al. ref. 8)

density field techniques (schlieren, etc.), line absorption, chromatography, electron microscopes, etc., have been used in recent years. Kubota and others used a combination of very fine (4 micron bead) thermocouples and high speed infra-red photography to study the site and mode of action of platonizers in double base propellants [Ref. 7]. Murphy and Netzer [Ref. 9] used a mercury arc source schlieren system for AP and AP-binder sandwich combustion studies. Klahr and Netzer further attempted the use of an argon (CW) laser source schlieren with either a neutral density wedge filter or a knife edge to study a variety of solid propellant combustion [Ref. 10]. Developments in laser light source optical systems, including schlieren, have been reported by Lu [Ref. 11] and Oppenheim [Ref. 12]. These systems are potentially valuable tools for propellant combustion studies. A combination of high speed photography (with other than laser light sources) and/or detailed surface study of thermally or depressurized quenched samples with a scanning electron microscope or other electron microprobe analysis have been reported by a number of researchers including Boggs [Ref. 3], Boggs and Kraeutle [Ref. 14], Derr and Boggs [Ref. 15], Boggs and Zurn [Ref. 16], Hightower and Price [Ref. 17], Varney and Strahle [Ref. 18], and Strahle, Handley and Kumar [Ref. 5].

Using an optical system of some type to study propellant combustion in a high pressure atmosphere provides a unique

opportunity for a "stop action" observation as well as continuous slow motion study of the flow field and surface configuration. Further, a well designed optical scheme has little effect on the combustion mechanism, which is particularly important when the boundary conditions are significant, as is the case when small samples are tested in small pressure vessels. Although highly attractive, particularly from a qualitative analysis standpoint, optical systems have several significant disadvantages when applied to combustion studies. The problems tend to fall into two areas: problems associated with the combustion system or mechanism itself and those associated with the optics system, independent of any particular item in the test section.

Combustion products, particularly smoke, accumulating within the combustion bomb or immediately above the burning surface can scatter or absorb light and generally obscure the surface action as well as degrade schlieren observations. Too low a purge rate allows too much smoke to accumulate while purging too rapidly might cause a large convective heat loss, thus affecting the combustion mechanism itself.

A major problem in observing surface reaction and the gas phase just above the surface during high pressure combustion of certain propellants is the visible light or self-luminous interference effects from the combustion zone. As the pressure is raised, the combustion zone tends to move closer to the solid surface and the problem is magnified.

This interference overpowers schlieren observations resulting in a yellow overtone in color photography or a washed out region in black-and-white [Refs. 10 and 11]. With an unlimited light source power supply, it is conceptually possible to simply overpower the interference but at the potential risk of affecting the combustion mechanism if the source intensity is high enough to cause heating of the specimen or the flow. A second and preferable potential solution is the use of the monochromatic properties of laser light and a narrow-pass filter combination with the filter at peak transmission at the laser wavelength [Ref. 11]. The wavelength of the laser and filter should be significantly displaced from the expected peak of the self-luminous interference.

In order to create a controlled steady state high pressure environment, a secure pressure vessel complete with viewing ports, ignition system and exhaust/purge facilities is required. The optical quality of the vessel windows must necessarily be high, particularly for a laser light source, and their physical strength sufficient to withstand the intended pressures. The internal dimensions of the chamber must be sufficient so as not to constitute an adverse boundary condition and unduly influence burning. The possibility for equipment failing under high pressure operation imposes additional safety precautions such as a remote control console from which the experimental runs may be initiated.

The techniques of ignition must include a minimum interference effect on the combustion mechanism. It is possible to create a heat sink if the specimen mounts or ignition system members are too massive or too close to the specimen, thus altering the burning. It is also highly desirable to have as even ignition as possible across the regression surface of the specimen.

Motion picture systems for data recording offers the possibility for both "stop action" as well as slow motion study of the flow field without interfering with the combustion process. Other methods, such as quenching, may actively interfere with the process while Q-switching laser techniques do not provide for continuous observation. Probes or fine wire thermocouples are also used but must be precisely positioned and represent a possible discontinuity during the burn. For motion picture recording, the light source must be of sufficient power for the desired beam geometry to enable film exposure at the necessarily high framing rates. The power levels for Q-switching techniques present no problems but for CW lasers in the visible spectrum the power levels are limited and the efficiencies low. The losses from each member of the optics train must also be considered in order to yield the necessary light intensity at the film plane. High ASA ratings for high speed films and developing methods to extend the ASA ratings may assist for lower light levels. Due to the time required for the

camera to accelerate the film from rest to the selected framing rate, it is essential that the ignition and camera initiation be fully coordinated to account for the propellant burn time at the seclected pressure and the available film length. This necessitates some method of viewing the specimen from the remote control console.

Specimen purity, construction and mounting techniques may add variables into the results. Intergranular cracks in polycrystalline propellants or fractures in single crystal specimens may represent discontinuities in the combustion process. For ammonium perchlorate especially, contaminants such as water necessitate special storage and handling. The specimen plane must be carefully positioned in the test section perpendicular to the optical axis to avoid additional problems in defining a focus reference point.

The test section for high pressure combustion studies is defined by the internal dimensions of the pressure vessel. The objective in the schlieren approach is to observe gradients in a single plane and preferably in a single direction. The flow field, however, is three-dimensional and the axial thickness of the field results in an averaging effect over the length of the test section.

The specimen has a known finite thickness in the axial direction. Depending on the criticality of focus, some reference point definition is required. The axial thickness variation of the gas phase with height above the burning

surface should be considered in focus point definition. The axial thickness of the gas phase is probably closest to that of the specimen nearest the burning surface. Simultaneous good focus of both the solid and gas phases, as well as obtaining the desired magnification, can be a major problem.

Interaction of coherent monochromatic laser light with the conventional knife edge produces diffraction patterns which render this combination unsuitable for laser schlieren systems [Ref. 11 and 12]. The inherent fringing around the periphery and general inhomogeneity of the laser beam may require it to be "cleaned" by spatial filtering or other techniques in order to be suitable for use in a schlieren system. Unmodified laser beams and the benefits of spatial filtering are discussed and illustrated by Klein [Ref. 13]. The plane polarized characteristic of laser light allows the use of optically active crystals to replace the conventional knife edge and thus to minimize or eliminate the associated diffraction patterns. The major advantage, however, is derived from the monochromatic nature of laser light which permits the use of a narrow-pass filter to minimize or eliminate the problem of self-luminous interference and observe only the schlieren. An additional advantage of a laser source is the dual use with a hologram setup or other dual system as reported by Lu [Ref. 11].

Of the available references to date, the combination of a CW laser source schlieren system with an optically active

quartz prism-polaroid sheet combination aperture for application in solid propellant combustion study has not been reported. The major objective of this thesis is to report on the development of a laser schlieren (optically active aperture) system designed to eliminate the problem of self-luminous interference during flow field studies and to apply it to the study of combustion of certain propellants at pressures to 2500 psi. The technique offers the potential for gas phase combustion study by the elimination of the self-luminous interference problems, while providing the qualitative flow field data of the schlieren method and retaining the overall advantages of high speed photography. In order for this combination to be a viable system, it must first overcome some inherent laser optics problems and provide a quality and sensitivity of schlieren comparable to conventional systems.

II. EXPERIMENTAL APPARATUS AND PROCEDURES

A. APPARATUS AND THEORY OF OPERATION

Basically, the optical system employed consisted of a CW argon laser source schlieren using high quality lenses, an optically active aperture in place of the conventional knife edge and a bi-concave lens to initially diverge the laser beam.

The schlieren aperture used was an optically active 30 degree quartz single-crystal prism and polaroid sheet combination to replace the knife edge. The commonly accepted theory of optical activity and optically active materials has been attributed to Fresnel (1825) and may be found fully described in Refs. 19-24. Very briefly, optical activity is the phenomenon displayed by certain crystals and solutions which rotate the plane of vibration of polarized light. The fundamental cause of optical activity in crystals is the atomic arrangement in like-handed spirals along the direction of propagation of the light. This direction is known as the optically active axis. The amount of rotation depends on the optically active material (i.e. quartz or cinnabar etc.), the wavelength of the light and, to a smaller degree, the temperature. The crystalline structure of quartz (silicon dioxide) has been described by Bragg and Claringbull [Ref. 25].

The amount of rotation by optically active quartz is strongly dependent on the wavelength, and is linear with distance along the optical axis. That is, given the wavelength and temperature, the specific rotation (degrees/mm) is a constant. A summary of the data collected [Refs. 19-22, 24 & 26) may be found in Table I . The data were used to obtain polynomial curve fit equations for the specific rotation as a function of wavelength and as a function of the inverse square of wavelength. These data approximations are plotted in Fig. 6 using the polynomials presented below.

TABLE I
Specific rotation of quartz

ϕ_s(deg/mm)	λ Å	$\beta(\lambda^2 \times 10^8)$	ϕ_s	λ	β
201.9	2265	19.492	29.73	5086	3.866
153.9	2503	15.958	27.46	5270	3.601
95.0	3034	10.863	26.5	5351	3.492
72.45	3404	8.632	25.54	5461	3.354
50.98	3969	6.348	22.1	5890	2.883
48.95	4047	6.107	18.0	6438	2.413
47.4	4102	5.943	17.26	6563	2.322
42.37	4308	5.388	16.54	6708	2.222
41.55	4358	5.265	15.55	6867	2.121
35.6	4678	4.569	13.9	7281	1.886
32.75	4861	4.232	11.59	7948	1.583

(data from refs. 19-21, 24&26)

Specific rotation versus wavelength: Wavelength in angstrom units, Å, and specific rotation in degrees/mm along the optical axis.

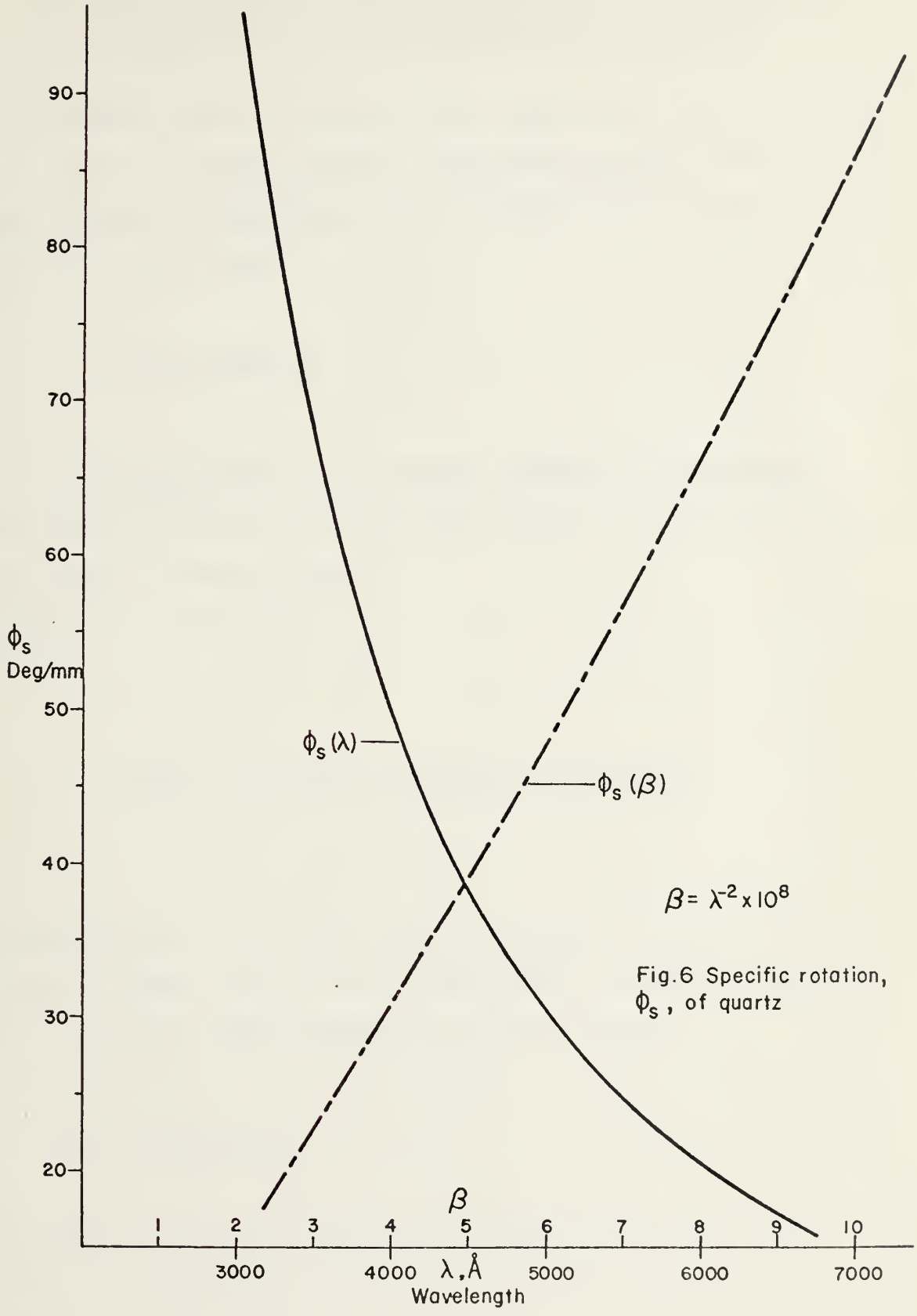

Fig.6 Specific rotation, ϕ_s, of quartz

$$\phi_s = 6095.07 - 8.82083\lambda + 5.78014E\text{-}03\,\lambda^2 - 2.1837E\text{-}06\,\lambda^3 + 5.14734E\text{-}10\,\lambda^4 - 7.71202E\text{-}14\,\lambda^5 + 7.15329E\text{-}18\lambda^6 - 3.75069E\text{-}22\,\lambda^7 + 8.5066E\text{-}27\,\lambda^8$$

Maximum error = 0.45°/mm over the range from 3000-7000 Å. Over the visible range, from approximately 4000-7000 Å, the following polynomial gives an excellent fit with errors of 1.3°/mm or less:

$$\phi_s \cong -2.10 + 8.14E{+}08/\lambda^2$$

Specific rotation vs. inverse square of wavelength:

Wavelength in angstrom units and specific rotation in degrees/mm along the optical axis.

Define: $\beta = \lambda^{-2} \times 10^8$

$$\phi_s = -0.282154 + 7.30959\beta + 0.105328\beta^2 + 2.65491E\text{-}03\,\beta^3$$

Maximum error = 0.37°/mm over the range 2.0-10.5. Over the visible range, 2.04 to 6.25, the plot is nearly linear and may be closely approximated by the following:

$$\phi_s \cong -2.328 + 8.34\beta$$

The errors for this approximation are less than 0.38°/mm.

The plane polarized nature of laser light permits the substitution of an optically active quartz prism-polaroid sheet combination for the knife edge as the schlieren aperture. Quartz is only one of several optically active materials that could be used. Parallel rays passing through a flow field with density gradients are differentially refracted resulting in a shift of position of impingement on the perpendicular face of the quartz prism. With a knife edge, either more or less light is allowed to pass, depending on the direction of the shift. The corresponding light or dark zones from the typical schlieren record. In the case of a quartz prism, the displaced light travels through differing thicknesses of quartz which in turn rotates the plane of polarization by differing amounts. The polaroid acts as a filter to pass rays whose rotation is close to the polaroid orientation and absorb the others. Again, the corresponding light and dark zones form the schlieren record. In order to avoid the deflection of the entire beam after passing through the quartz prism, a second complimentary but optically neutral prism of matching index of refraction is necessary [Refs. 11 and 12]. Figures 7 and 8 show the geometric relations of displacement to rotation and the qualitative ray tracing through the prism system.

The completed optical system is shown in Figs. 9 and 10. The laser source beam was diverged by a bi-concave lens to the desired diameter at the first schlieren lens. The

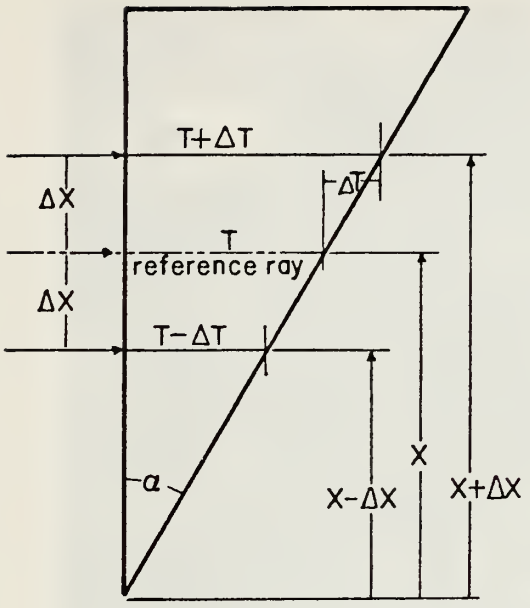

$\Delta X = f_2 \epsilon$ - refraction displacement

$\Delta T = \tan(\alpha) \cdot \Delta X$ - diff. thickness

f_2 - focal length of second schlieren lens

ϵ - total refraction

Fig.7 Geometric relationship of differential thickness, ΔT, to refraction displacement, ΔX

n - index of refraction

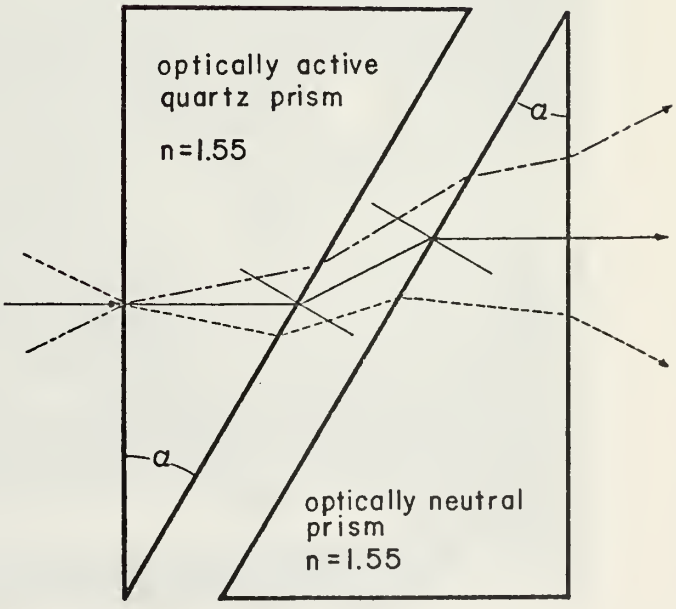

Fig.8 Qualitative tracing of converging beam through two prisms

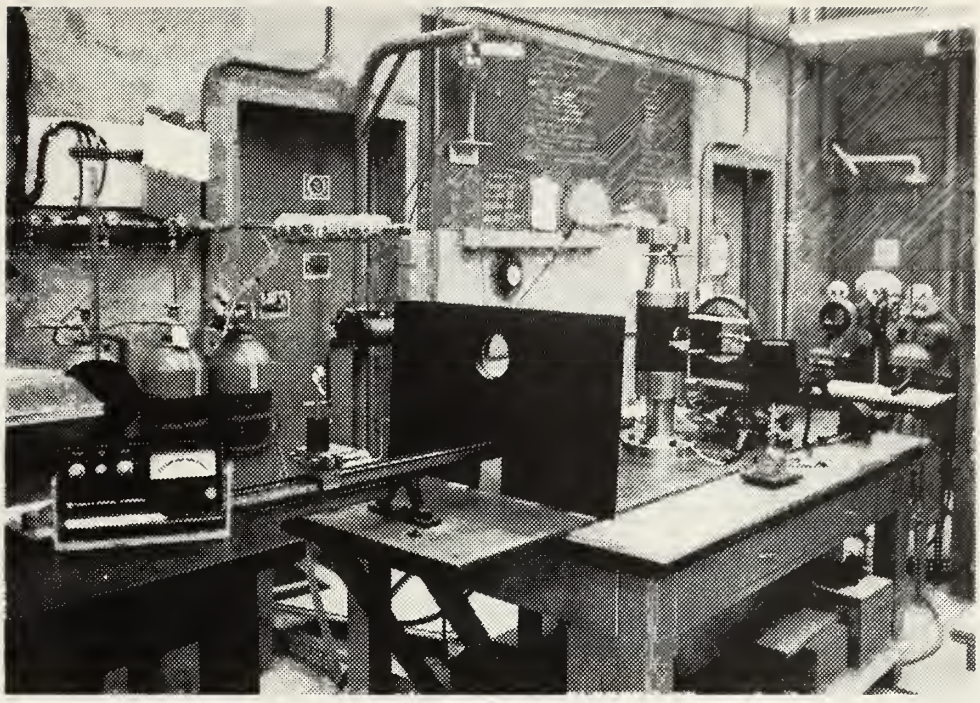

Fig.9a. General layout of schlieren system

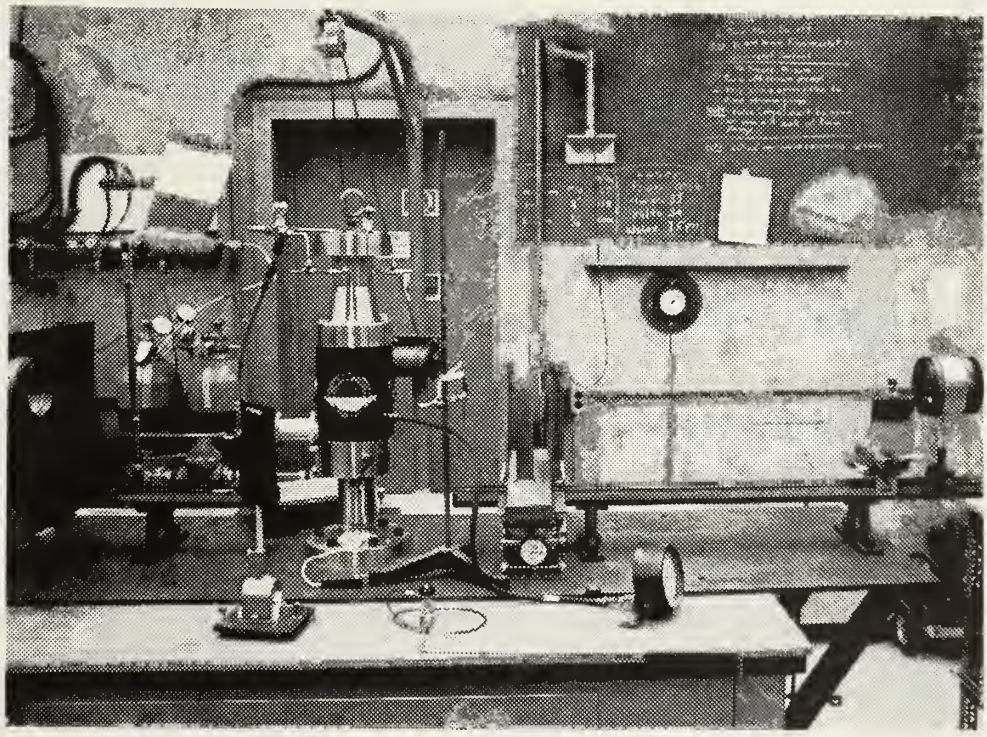

Fig.9b Side view of schlieren system from lens L_1 to lens L_3

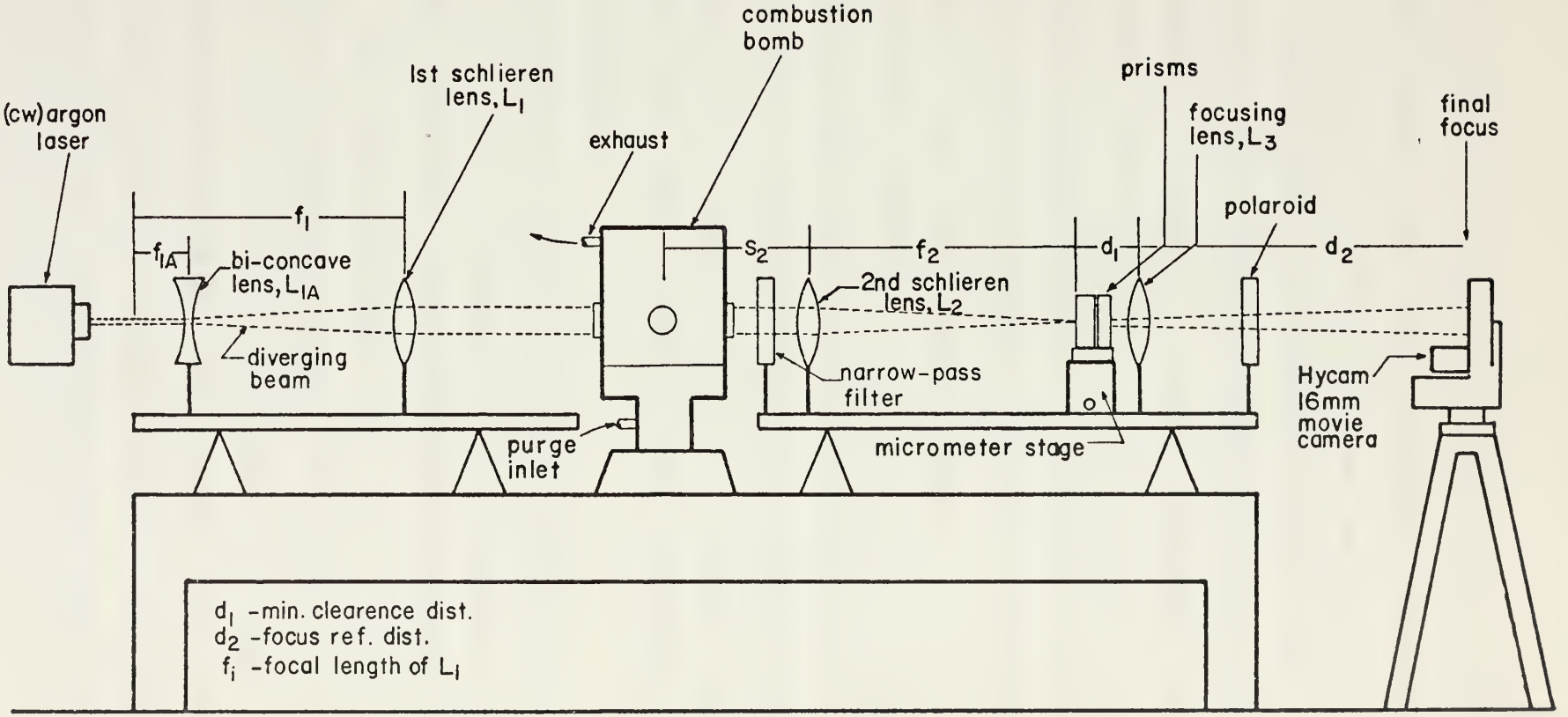

Fig.10 General laser schlieren system
(side view)

focal points of the first schlieren lens and bi-concave lens were coincident. The first schlieren lens collimated the beam and directed it through the test section, the narrow-pass filter and on toward the second schlieren lens. The second schlieren lens focused the quasi-parallel beam from the test section to a point in a plane coincident with the perpendicular face of the single-piece quartz crystal. The light passed through the quartz prism and correcting prism, through the polaroid sheet, and was focused onto the film plane by the final focusing lens..

The light source used was a Control Laser continuous wave (CW) argon laser, model 902A, operating at the 4880 Å line. The laser was operated at 32 amps/220 vac to deliver a maximum power of 1.3 watts at 4880 Å. The beam width was 2mm at the $1/e^2$ intensity point with a divergence (full angle) of 0.6 milrad.

The positioning of the two schlieren lenses and the final focusing lens was determined from laboratory space considerations and by the final image size desired on the film plane. The thin lens model, $1/F = 1/S + 1/S'$, was used to position all optical lenses. The final focal plane for the entire system was calculated using the model to find the approximate position. The physical size limitations of the laboratory would have forced "folding" the optics several times to fit, if a real image system were to be used. In order to shorten the optics and still achieve the desired

final image size near 1.0 magnification, the second schlieren lens was placed such that the test section was inside its focal point. The virtual image thus created by the second schlieren lens was used as the object for the final focusing lens. Figs. 11 and 12 show the approximate layouts for the real and virtual image systems for a final magnification of near unity based on the thin lens assumptions.

The thin lens model can be non-dimensionalized to obtain a direct relationship for object distance to image distance in terms of focal length, f, as shown in Fig. 13a & 13b.

All photographic records were made directly onto the film plane. The omission of the camera lenses reduced the complexity of the optical problem and minimized further light losses. Initial system evaluation was done by taking long exposure schlieren pictures of laminar flames. They were made using a Leica (model M-2) camera and Tri-X 135 panchromatic film (ASA 400). Exposure times of 2 millisecs produced satisfactory results. For motion picture recording, a Hycam model K2004E-115 high speed 16mm motion picture camera was used. Framing rates of up to 10,000 frames/second were used with exposure times of 80 microsec or less depending on the associated shutter used. The lower limiting time capability was 1 microsec. Movie film types included 7277 4X reversal (ASA 400), 2475 Estar-AH base (ASA 1000) and 7224 negative (ASA 500). The 7277 4X was used primarily because it has a color sensitivity peak in the blue-green.

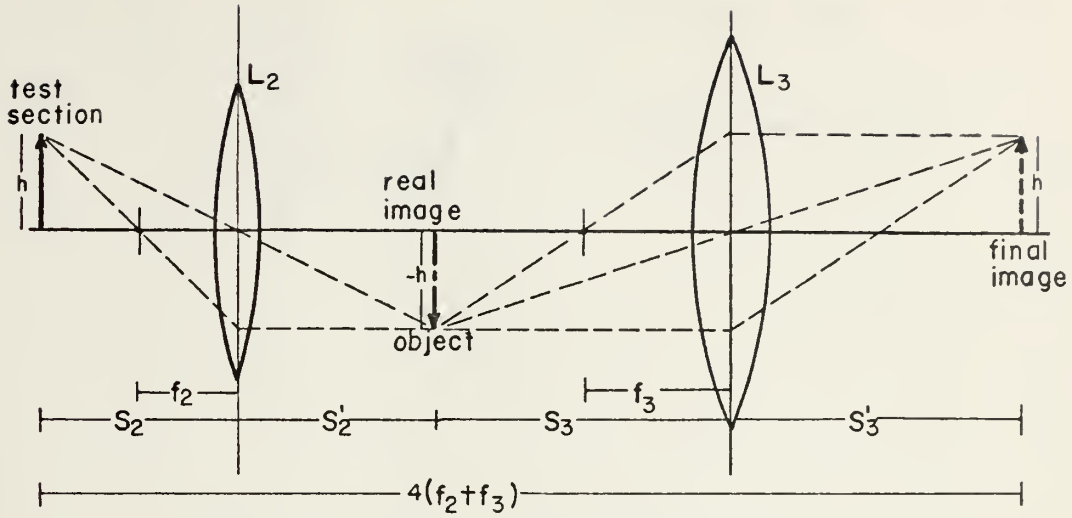

Fig.11 Real image setup ($S_2 = 2f_2$ & $S_3 = 2f_3$)

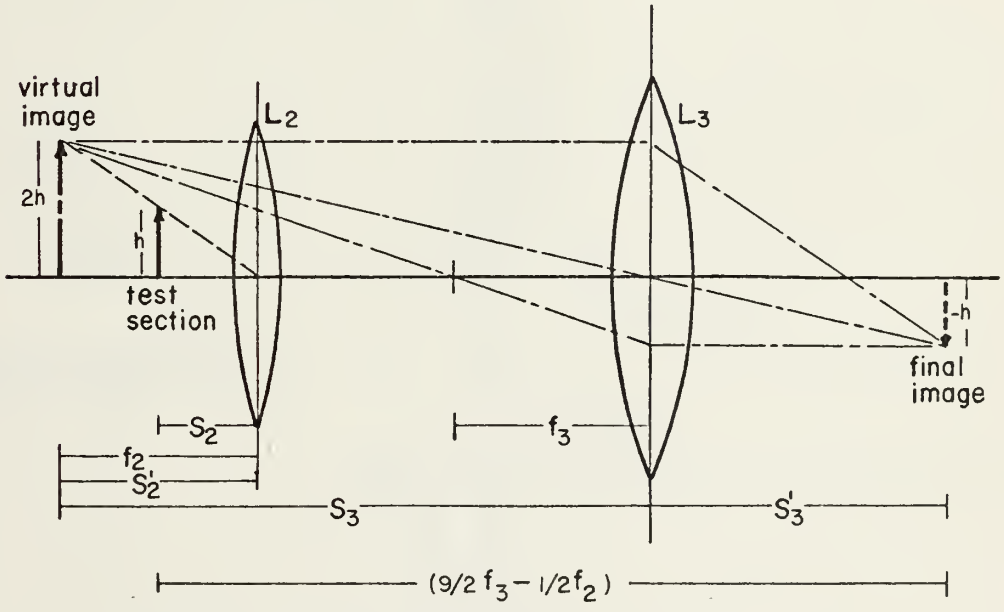

Fig.12 Virtual image setup ($S_2 = 0.5\, f_2$ & $S_3 = 3f_3$)

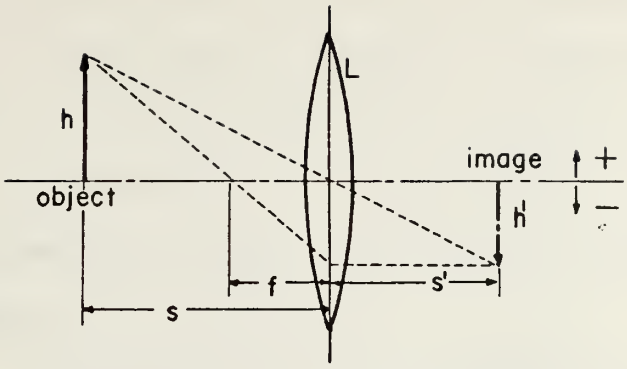

$1/f = 1/S + 1/S'$

$m = h'/h = -S'/S$

Fig.13a Thin lens model

$X = S/f$

$X' = S'/f$

$X' = \frac{X}{X-1}$

Fig.13b Non-dimensional thin lens model

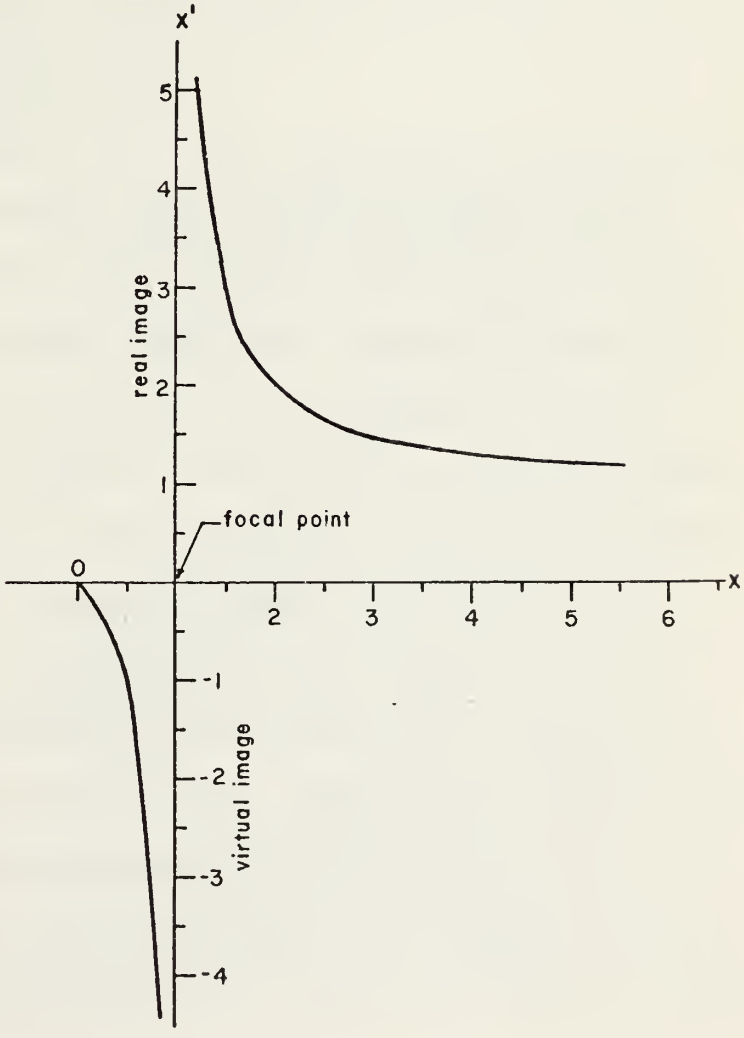

A Red Lake Millimite TLG-4 oscillator was used during all movie runs to provide a timing mark on the film edge at the pre-selected time intervals.

The 4880 Å narrow-pass filter was located immediately downstream of the test section, prior to the second schlieren lens.

In the test section, facilities were provided for mounting either of two pressure vessels used for high pressure propellant combustion. Each combustion bomb was connected to a common ignition system as well as to common plumbing for the nitrogen pressurization source and smoke purging system.

The low pressure bomb, Fig. 14a, was made from 300-series stock steel with an internal test section diameter of 8.0 cm and walls 4.5 cm thick. Photographic viewing ports 2.54 cm in diameter and oriented along the axis were fitted with plate glass windows 3.2 cm thick. An additional viewing port was located on the side of the bomb for ignition-camera initiation coordination. The low pressure bomb was pressure tested to 1500 psi but limited to operation at 800 psi.

The high pressure bomb, Fig. 14b, was fabricated from #347 stock steel and likewise fitted with two viewing ports along the axis and one on the side. The internal test section diameter was 5.0 cm and the walls 5.05 cm thick. Due to the maximum operating pressures of 3000 psi, the viewing diameter was reduced to 1.27 cm and made from schlieren quality neutral

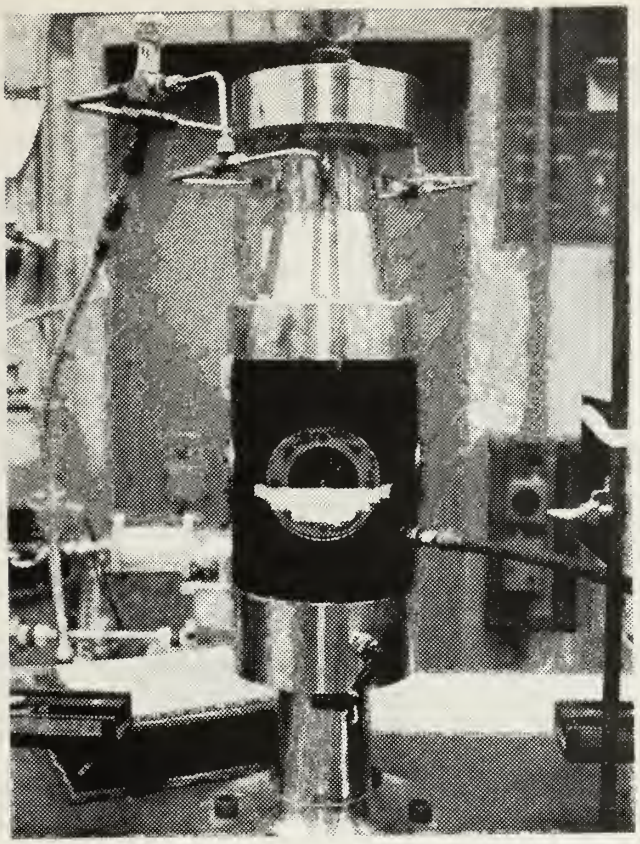

Fig. 14a Low pressure combustion bomb (800psi)

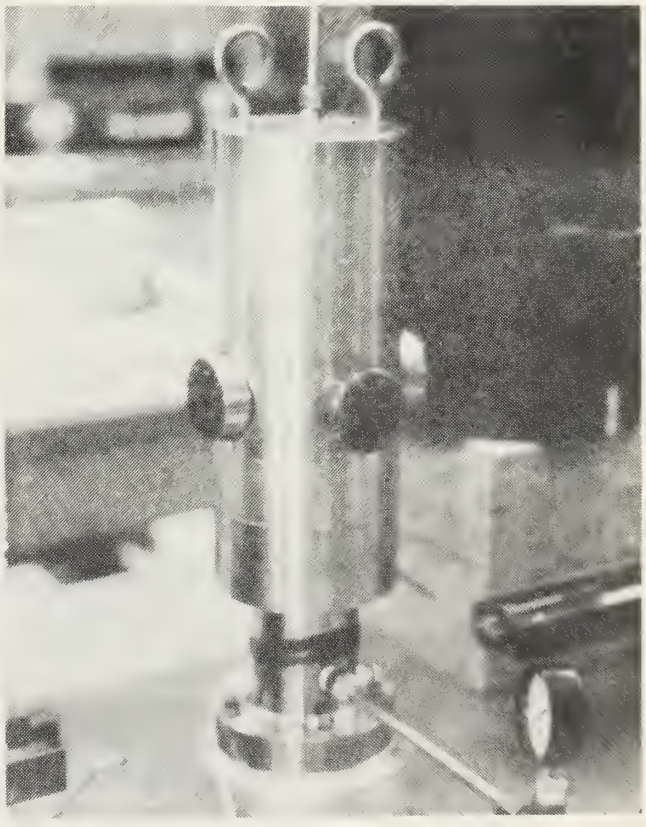

Fig. 14b High pressure combustion bomb (3000psi)

quartz 3.2 cm thick. The high pressure bomb was pressure tested to 4500 psi prior to any experimental runs. As an added safety precaution for the very high pressures, a steel shroud was fitted to surround the entire bomb during a pressure run.

To accommodate the change of window diameter between the two bombs and to achieve as little light loss as possible, two bi-concave lenses were used as follows: 5.0 cm focal length lens for the low pressure bomb to give a test section beam diameter of approximately 2.59 cm; 10.0 cm focal length lens for the high pressure bomb with a beam diameter of about 1.3 cm.

The remote control console provided for complete control of system pressurization, ignition and camera initiation. The location of the console was out of the line of sight through the windows, in the event of failure. A surveyor's transit and first-surface mirror provided pre-ignition observation of the specimen for camera coordination.

The ignition system consisted of two electrodes mounted on either side of the specimen pedestal. Between the electrodes a #32 nickel-chromium wire was pulled taut across the upper specimen edge and secured to each side. The ignition wire was electrically in series with a variable resistor in order to control the current provided by the 12 VDC battery source. A continuity check circuit with a visual indication was also included. Figure 15 shows a specimen.

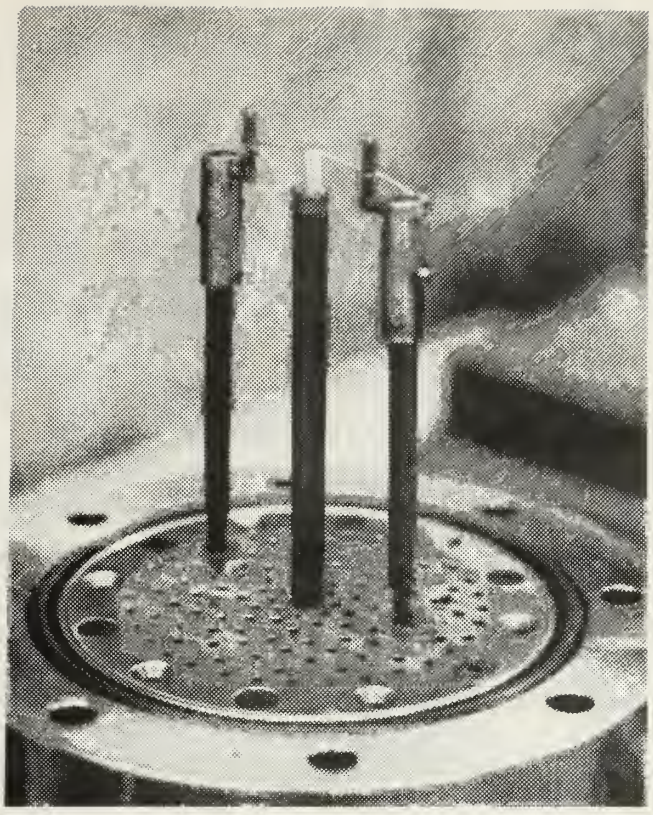

Fig.15 Typical specimen mounted for ignition

The pressurization/purge system was controlled from the remote console through a dome valve. This dome valve in turn controlled the flow from the compressed gas resevoir, nitrogen in this case. A pressure tap and gauge read the bomb pressure directly and was viewed from the console. Exhaust port valves on the top of the bomb controlled the rate of the exhaust flow for smoke removal. The exhaust flow was introduced through a porous plate in the bottom of the chamber, passed up through the test section and then vented to the atmosphere.

B. EXPERIMENTAL PROCEDURES AND PROBLEMS

1. Introduction

A three-phase test plan was developed in order to provide an opportunity to improve techniques and to compare the intermediate results with the conventional schlieren systems.

The first phase was for initial system setup, familiarization and development. Items such as city gas diffusion flames, candle flames and bunsen burners were used at atmospheric pressure for basic quality and sensitivity comparisons with previously reported systems. Initial results showed enough potential to continue with the second phase.

The second phase of the test plan was to duplicate portions of the solid propellant combustion study reported by Murphy and Netzer [Ref. 9] and Abraham, Klahr, Gerhardt and Netzer [Ref. 10] for direct comparison of sensitivity, quality and feasibility using identical specimen/environments with two different optical systems. This phase was a most important preliminary to the ultimate intended use of the system for high pressure propellant combustion study. This phase also assisted in technique development and identified component influence (i.e. polaroid) on sensitivity and quality. The criticality of the system final focus was also demonstrated. Additionally, these intermediate results

supported the feasibility of this laser schlieren technique for the third and final phase.

The final phase was to apply the system to combustion phenomena which could not be readily studied using conventional schlieren techniques. More specifically, ammonium perchlorate deflagration was examined to pressures of 2500 psi.

2. Initial System Setup

The optical bench and combustion bomb pedestal mounts had been sight aligned and leveled, then hard mounted on a common steel sheet for previously conducted experiments. All additional optical members used in this system were aligned to this basic reference. In general, it was found that the overall alignment of the system was critical for obtaining good results. Initially, only the laser and the two schlieren lenses, L1 and L2, were used for alignment (see Fig. 10). With the laser leveled, visually aligned to the bench and adjusted to the desired test section center height, the first and second lenses were mounted in place such that the laser beam impinged on each lens at its center without being refracted off the optical axis of the bench. Each additional optical member was added one-at-a-time and aligned to the reference bench axis separately. Fine adjustments to the bi-concave lens, L1A, were necessary to select and position a clean portion of the expanded laser beam to achieve optimum specimen illumination.

The CW argon laser used (Control Laser model 902A) was tuned to 4880 Å using the combination of optical power meter and visible blue-green color characteristic. 4880 and 5145 Å were the two primary lines (max. power) of this model laser. The 4880 Å line and matched narrow-pass filter combination was specifically selected to move as far as possible in the electromagnetic spectrum from the expected wavelengths of 5100+ Å for self-luminous interference. Other laser lines below 4880 Å did not provide sufficient power to be considered.

System focus proved, initially, to be a problem and, overall, to be critical for reasonable resolution. The lens system was set up using the thin lens model. The positioning of the second schlieren lens relative to the test section took the final image size into account. During this initial setup, the filter, polaroid sheet and prisms were not considered or included. Final focusing was accomplished with all the optical members in place: bi-concave lens, L1A, first schlieren lens, L1, two bomb windows, narrow-pass filter, second schlieren lens, L2, both prisms, polaroid sheet and the final focusing lens, L3 (see Fig. 10). The final focal plane was identified relative to the reference of the final focusing lens. A small white screen was used to observe the focus of a fine wire loop in the center of the test section. The criterion for "in focus" was the wire appearance to the eye of two observers as the screen was

moved axially. The calculated and apparent final focal planes differed by a few centimeters but this was attributed to the thin lens model shortcomings, applied to non-thin lenses, and failure to account for the prisms, polaroid, filter or bomb windows' effects. The specimen magnification in the final focal plane was approximately 0.85.

Initially a spatial filter was used to "clean" and diverge the beam prior to the first schlieren lens. In this arrangement, the pinhole plane was located at the focal point of the first lens. The combination of power losses across the filter itself and the large divergence angle made it impossible to expose the film (7277 4X reversal ASA-400) at or above 2000 frames per second. A satisfactory substitution was found using a bi-concave lens prior to the first schlieren lens, with the two focal points coincident. The bi-concave focal length coupled with that of the first schlieren lens controlled the beam geometry at the first lens and, consequently, through the test section as indicated in Fig. 16. By minor adjustments of lens L1A, a usable portion of the beam could be placed on the target element without further beam filtering.

Tuning the system to the best schlieren response was largely a matter of finesse and involved adjusting the combination of quartz prism and polaroid. Initially, the polaroid was adjusted (without the prisms or bomb windows in place but all other optical elements included) for about

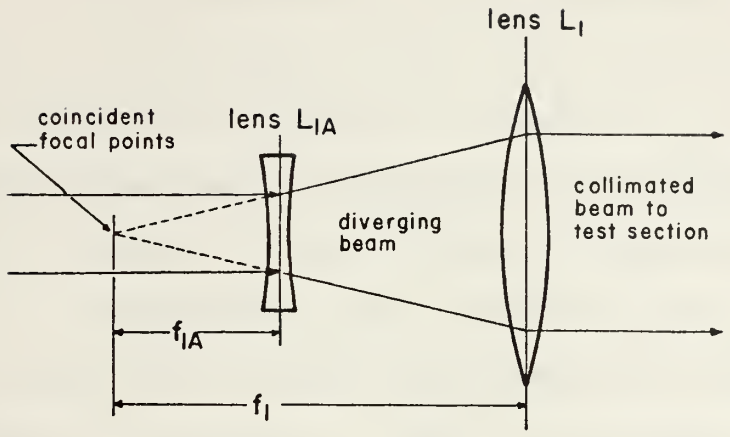

Fig.16 Divergence of laser beam

50% transmission. The prisms, mounted on a two-degree-of-freedom micrometer stage, were moved into place and fine adjusted until the desired schlieren contrast was produced. If the background changed and became too light or too dark, the polaroid was rotated slightly to a position of more or less transmission and the prism readjusted to obtain satisfactory schlieren. This tuning continued until the combination of good background and good schlieren were simultaneously produced. A good background was as uniform as possible, with the transmission level about half-way between the light and dark schlieren extremes. Prior to each combustion bomb run, the system was "tuned" using the laminar portion of a city gas diffusion flame.

3. Schlieren Sensitivity Matching

The sensitivity of any schlieren system is a function of the focal length of the second schlieren lens/mirror and the type and adjustment of aperture. The conventional knife-edge system has been described by Leipmann and Roshko [Ref. 27]. Figure 17 shows a typical test section.

Collimated light, passing through the test section, is refracted by spatial and temporal fluctuations in the index of refraction. Light is refracted toward an increasing density (positive density gradient). The density field which causes the index of refraction fluctuations is the result of the combustion physics of a given propellant under a specified pressure. In addition, effects from the exhaust system flow could be superimposed on the density field if the flow were too high. The total refraction, ε, of an individual ray of light is the sum of all incremental effects from entry to exit of the test section. Specifying the test parameters (i.e., propellant type, pressure, etc.) fixes the resultant total refraction. Thus, the net refraction is not available as a parameter for sensitivity or contrast control in the schlieren record. The more sensitive the schlieren system, the smaller the total refraction can be and still produce a detectable schlieren record.

The second schlieren lens/mirror focuses the quasi-collimated light from the test section to a point at the

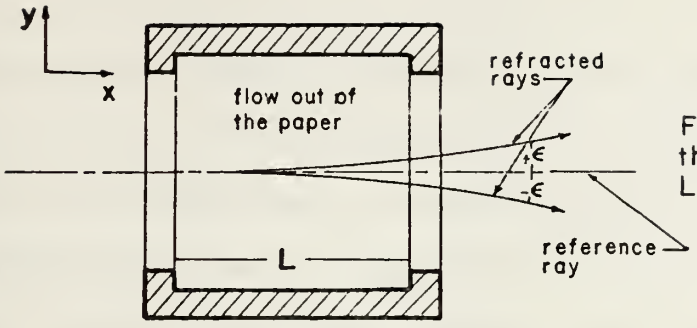

Fig.17 Refraction of light through test section(after Leipmann and Roshko ref.27)

$$\epsilon = \int_0^L \left[\frac{1}{n}\frac{dn}{dy}(x)\right] dx \cong \frac{\beta L}{\rho_s}\left(\overline{d\rho/dy}\right)$$

schlieren aperture. Refracted light rays are displaced at the aperture focus point relative to unrefracted or reference rays ($\Delta x = f_2\ \varepsilon$), proportional to the total refraction, ε, and the focal length of the second lens, f_2 (Fig. 7). The displacement, Δx, is directly related to sensitivity. The only positive sensitivity contribution of the second lens, therefore, is through its focal length, f_2. The lens can have a negative contribution from spherical aberrations if too small in diameter or if the beam is well off center. Non-uniformities in the glass may also degrade the resultant schlieren record.

The optically active aperture (quartz prism-polaroid) previously described controls both sensitivity and contrast,

assuming a fixed total refraction, ε, and a specified focal length, f_2. There are two major points which distinguish this aperture from the conventional knife edge. First, the polaroid sheet defines the light-dark extremes possible from the polaroid properties of transmission and absorption. With any combination of system optical members included, assuming the laser polarization is not destroyed, rotating the polaroid sheet will define the light-dark extremes possible in the schlieren record. Contrast in the schlieren record is defined by both the polaroid sheet and total system sensitivity. For a given density gradient, the combination of polaroid and system sensitivity will cause contrast of up to (but never exceeding) the light-dark extremes set by the polaroid alone. Second, it is possible to observe identical schlieren records for differing total refractions (density gradients). That is to say, there is a certain cyclic nature or periodicity associated with this schlieren aperture. The nature of the periodicity is dependent on the total system sensitivity and the relationship of reference ray polarization orientation to that of the polaroid sheet transmission axis.

The polaroid sheet has an axis of maximum transmission and, 90 degrees to it, an axis of maximum absorption. In general, the polarization orientation of the reference (or unrefracted) rays, after having passed through the prisms, should bisect the two axes of the polaroid sheet (Fig. 18a).

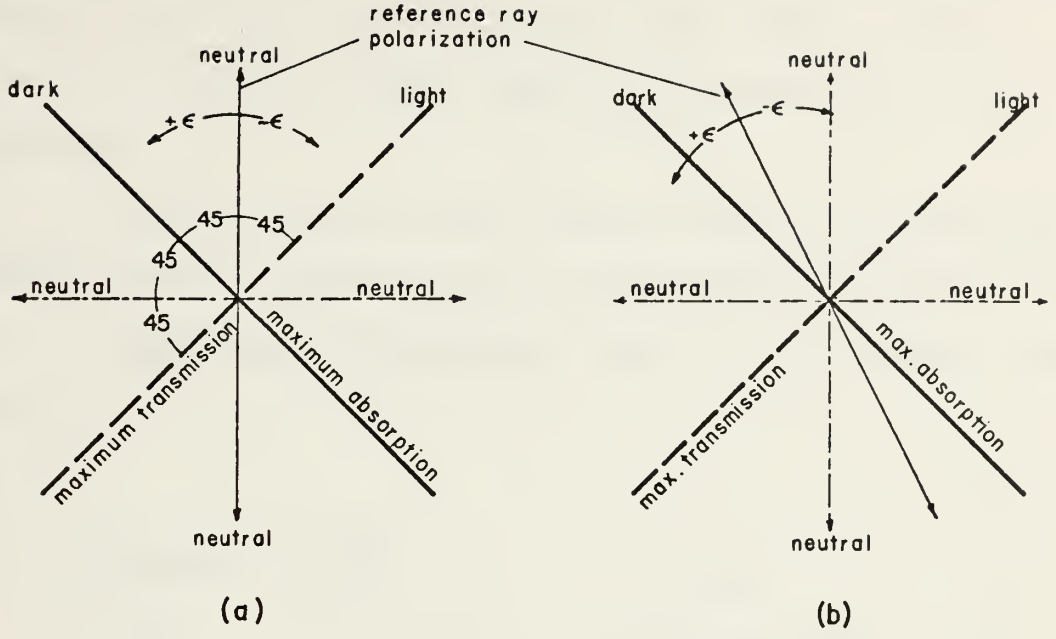

Fig.18 Polaroid sheet and reference ray polarization orientation

The reference could be along either bisecting axis. Ideally, the steepest density gradients in the flow field, coupled with the total system sensitivity, should cause a maximum differential rotation of ± 45 degrees for the refracted rays. This would correspond to the extremes of the light-dark and produce the optimum schlieren record. With the reference polarization as shown in Fig. 18a, increasing the sensitivity would cause a greater rotation for the same density gradients. If the deflected portion of the beam is rotated more than ± 45°, an erroneous reversal in the density gradient would

be indicated. This cyclic behavior becomes more critical in one direction if the reference axis and polaroid transmission axis are at other than 45° (Fig. 18b). This is sometimes necessary when a darker schlieren record is required.

Matching system total sensitivity to the expected maximum density gradients may be achieved as outlined below.

Derivation of Equations (see p. 8 for symbols and units):

$$\epsilon = \int_0^L \left[\frac{1}{n}\frac{dn}{dy}(x)\right] dx \cong \frac{L\beta}{\rho_s}\frac{\overline{d\rho}}{dy} \quad (1)$$

$$\Delta X = 10 f_2 \epsilon \quad (2)$$

$$\Delta T = \Delta X \cdot \tan(\alpha) \quad (3)$$

$$\Delta\Phi_f = \phi_s \Delta T \quad (4)$$

$$\Gamma \equiv \beta/\rho_s \quad (5)$$

$$\xi \equiv 10 f_2 \phi_s \tan(\alpha) \quad (6)$$

$$\Delta\Phi_f = \xi \Gamma L \left(\overline{d\rho/dy}\right) \quad (7)$$

Sample Calculations:

Consider a single perfect gas, N_2, in the test section in which the density gradients are caused only by temperature gradients (i.e., at constant pressure).

$R_{N_2} = \mathcal{R}/MW_{N_2} = 296.79$ j/Kg-°K $\qquad \rho_s)_{N_2} = p_s/R_{N_2}T_s = 1.25057$ Kg/m^3

$\beta_{N_2} = 2.97 \cdot 10^{-4}$ (ref.27) $\qquad \Gamma = 2.3749 \cdot 10^{-3}$ m^3/Kg

$\rho = \frac{p/R}{T} = \frac{\text{const}}{T} = 23.2311\, p/T$ (where pressure in psi) Kg/m^3

let $\quad \Delta\rho/\Delta y = (\rho_2 - \rho_1)/\Delta y = \frac{23.2311p}{T_1 \cdot T_2}(T_1 - T_2)/\Delta y \cong (\overline{d\rho/dy}) \frac{\text{Kg/m}^3}{\text{cm}}$

Estimates of $(\overline{d\rho/dy})$ for N_2 may be obtained from Fig. 19 from the estimated temperature field with the product of the temperature extremes, T_1T_2, as parameters. Knowing the density gradient allows tradeoffs in variables in the total sensitivity parameter, ξ, to achieve a $\Delta\Phi_t$ of ± 45 degrees or less (see Eqns. 6 & 7 above).

Example of Excessive Sensitivity (N_2 is the single perfect gas):

Given:

f_2 - 200 cm $\quad$ L - 2.0 cm $\quad$ α - 45°

Φ_s - 50 %/mm $\quad$ Γ - $2.375 \cdot 10^{-4}$ $\quad$ ξ - 10^5

$\Delta\Phi_1 = 47.498$ (cm-deg-m^3/Kg)$(\overline{d\rho/dy})$ $\frac{\text{Kg/m}^3}{\text{cm}}$

The results are plotted in Fig. 20 to show that a monotonic density gradient could produce "fringing". That is, erroneous changes in gradient could be inferred if sensitivity and gradients are grossly mismatched.

Fig. 21 shows the required total sensitivity to achieve a reference total rotation of ± 45 deg for a reference test section length of 1.0 cm.

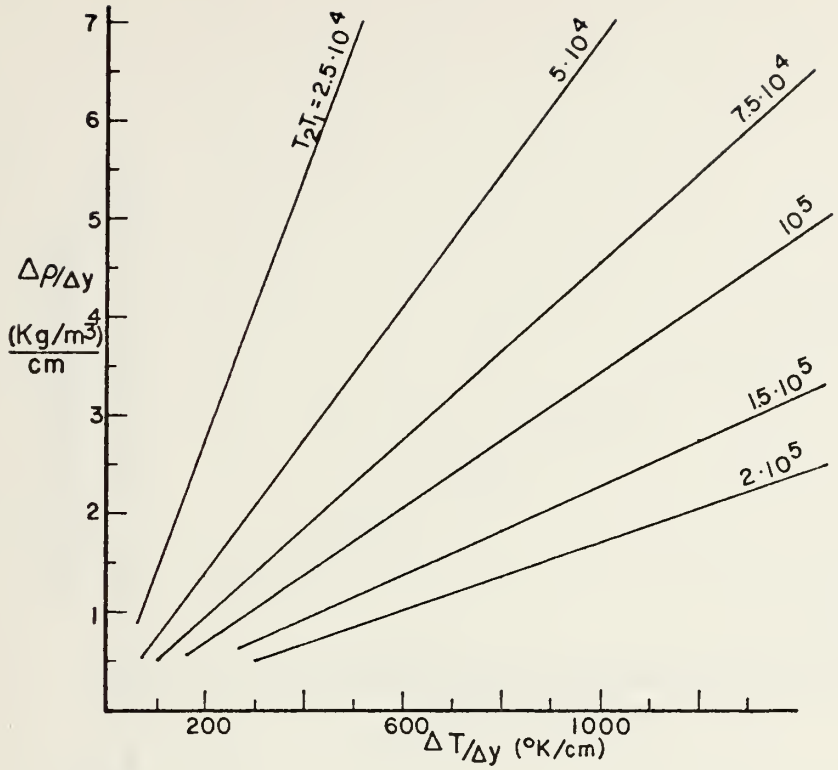

19a. P=14,696 psi

Fig. 19 Density gradients for N_2 in terms of temperature extremes

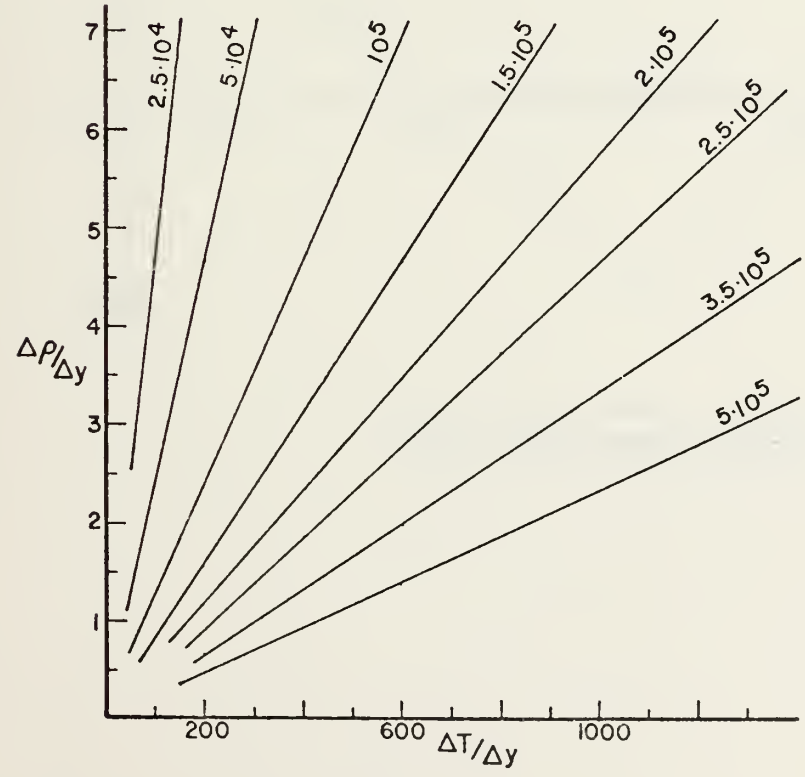

19b. P=50 psi

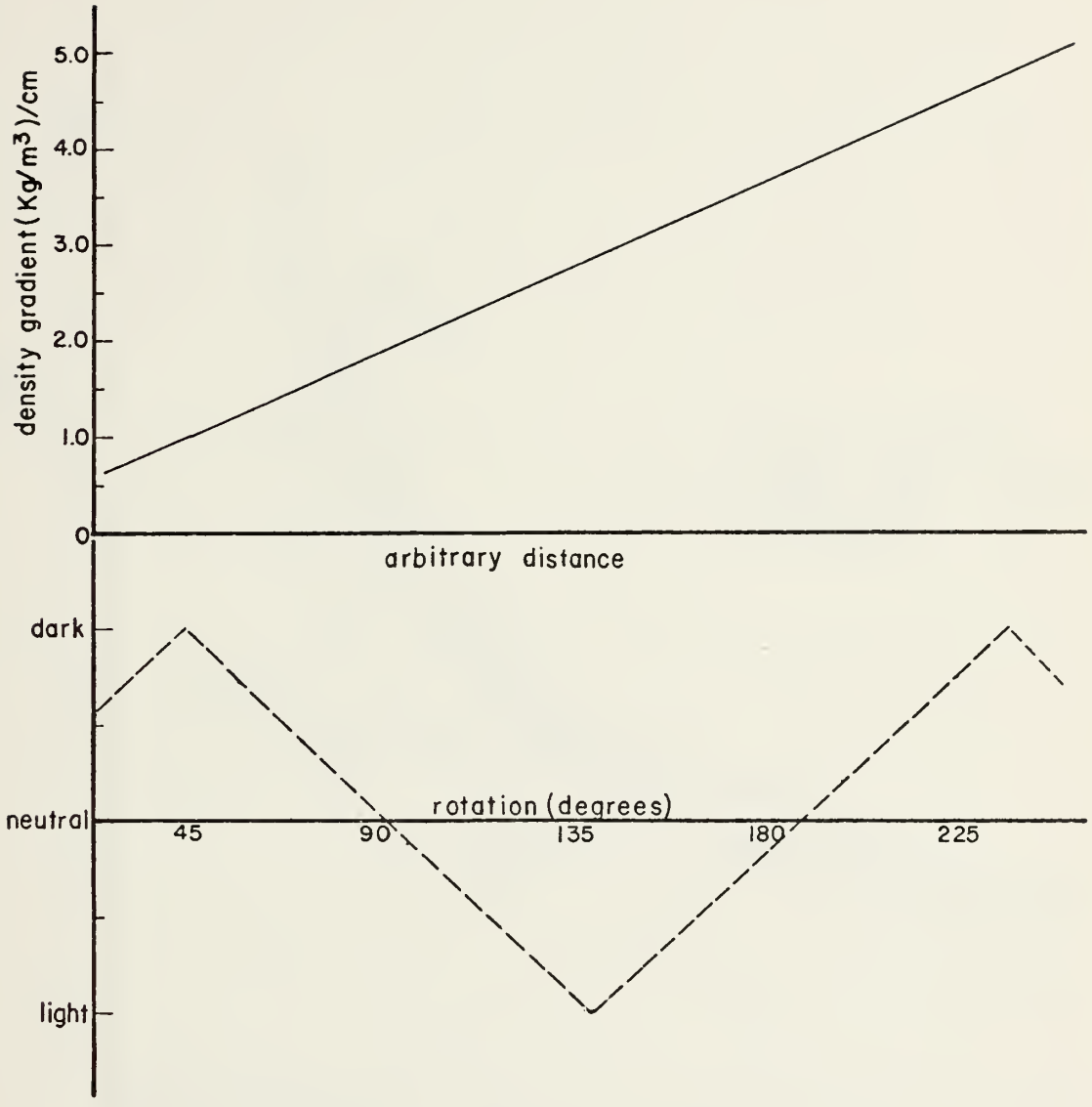

Fig.20 Cyclic intensity variation
with monotonic density gradient

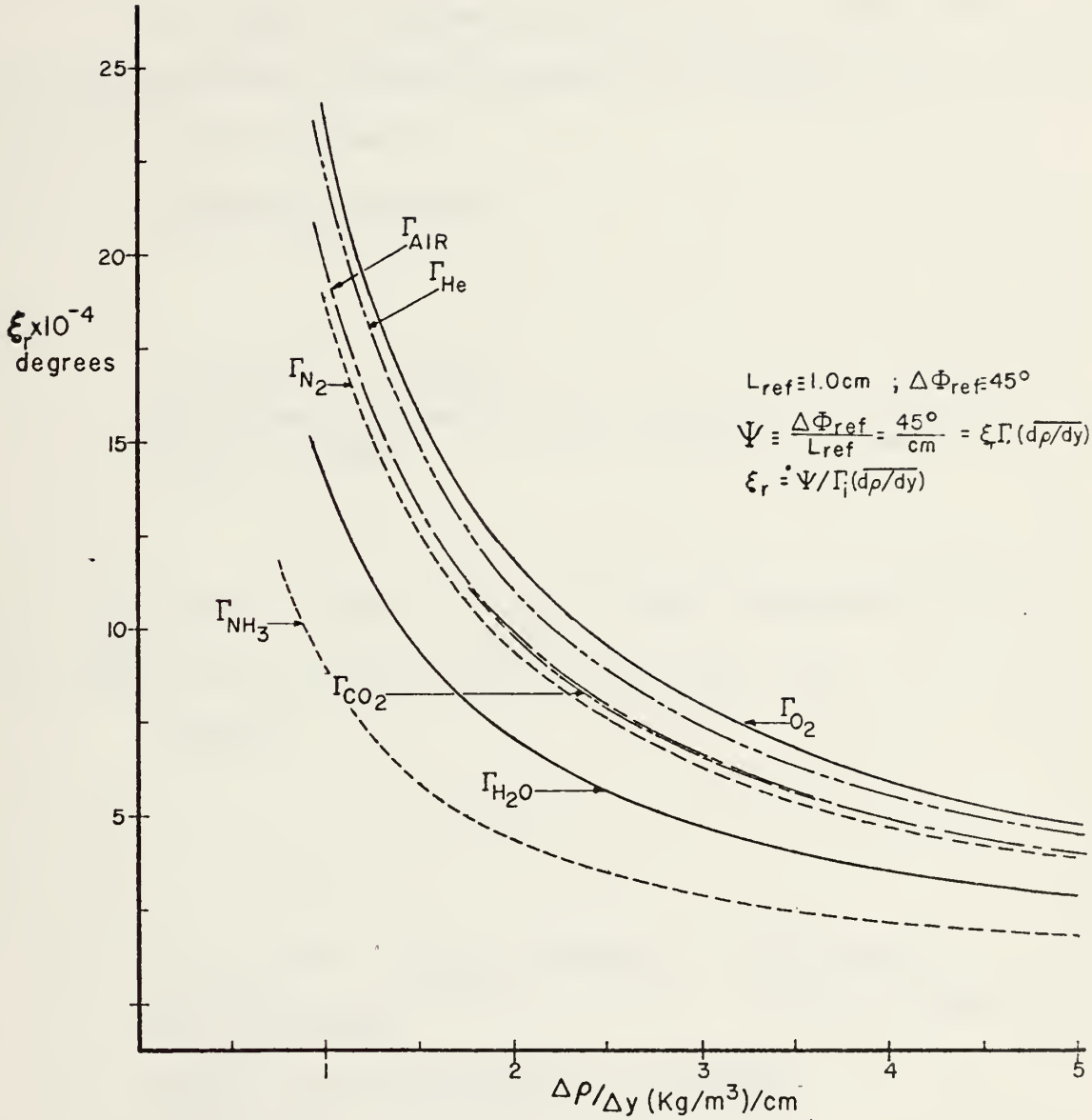

Fig.21 Required total sensitivity, ξ_r, to achieve reference rotation, Ψ

Thus, for the existing system, assuming a 1.0 cm test section length, nitrogen density gradients of 1.25 $(Kg/m^3)/cm$ would be required to produce ± 45° differential rotation.

In order to estimate some order of magnitude measure of the reported schlieren system performance, the following calculations were made.

System Parameters:

$f_2 = 86.0\,cm$; $\alpha = 30\,deg$

$\phi_s = 32.3\,deg/mm$; $\xi = 10 f_2 \phi_s \tan(\alpha) = 16038\,deg.$ - total sensitivity

$\Delta\Phi_f = \xi \Gamma L (\overline{d\rho/dy})$

A) Consider a candle diffusion flame temperature profile as reported by Gaydon and Wolfhard [Ref. 28].

Assume:

$p = p_s = 14.7\,psi$; $\rho_s = \rho_s)_{air} = 1.293\,Kg/m^3$; $\bar{\beta} = 3.50 \cdot 10^{-4}$

$L = 1.0\,cm$ $\Gamma = 2.71 \cdot 10^{-4}\ m^3/Kg$

$\Delta T/\Delta y = 3850\,°K/cm$

$\Delta\rho/\Delta y)_{max} = (const)\,p/T_1 T_2 (\Delta T/\Delta y)_{max} = 0.86 \frac{Kg/m^3}{cm}$

$\Delta\Phi_f = 3.7\,deg.$

B) Consider a standing normal shock wave in dry air (assumed thermally and calorically perfect).

$M_1 = 2.0$ $M_2 = 0.577$ let $\rho_{1t} = \rho_s)_{air} = 1.293\ Kg/m^3$

$\rho_1/\rho_{1t} = 0.23$ $\rho_2/\rho_1 = 2.667$ $L = 1.0\ cm$

$\Gamma = 2.56 \cdot 10^{-4}\ m^3/Kg$

$\Delta\rho/\Delta y = 49.6\ \frac{Kg/m^3}{cm}$ $\Delta y = 10^{-4}\ m$ (shock thickness)

$\Delta\Phi_t = 204^\circ$

C) Vertical smearing of the schlieren for AP combustion:

During the exposure time for any given frame, the hot gases have a vertical velocity which results in a "smearing" on the film. The smear is simply the distance a gas particle may move during the exposure time (smear = velocity times exposure time).

Assume: For pure ammonium perchlorate (AP) deflagration

1. The gas and solid phases have the same cross section
2. The combustion process is stoichiometric
3. The combustion is at constant pressure

$\dot{m}$ = mass burn rate = $(\rho \times \text{vol.})/\text{sec.} = \rho A_c r)_{solid} = \rho A_c \text{Vel})_{gas}$

$\rho r)_{solid} = \rho \text{Vel})_{gas} = (p/RT) \cdot \text{Vel}$

$\rho r)_{solid} = 1.95 \times 10^{-3}$ Kg/m^3 x 0.51cm/sec (at 500psi)

$$NH_4ClO_4 \longrightarrow 1.62H_2O + 1.015O_2 + 0.76HCl + 0.265N_2 + 0.23NO + 0.12Cl_2 + 0.12N_2O \text{ (Ref. 2)}$$

moles mix = $\sum_i \text{moles}_i = 4.13$; $y_i = \text{moles}_i/\text{moles mix}$

$MW_{mix} = \sum_i y_i MW_i = 95.3726$; $R_{mix} = \mathcal{R}/MW_{mix} = 87.1833$ j/Kg-°K

$T = T_{flame} \cong 1200$°K (Ref. 2)

$\text{Vel} = (\rho r)_{solid} (RT/p)_{mix} \cong 30$ cm/sec

smear at 80μsec = $2.4 \cdot 10^{-3}$cm (0.001in.) exposure time

The calculated smear was not considered significant for the near-surface gas phase observations.

4. Specimen Preparation and Mounting

A variety of specimens was used including ammonium perchlorate, both single crystal ultra-high purity (SC-UHP) and polycrystalline (PC-UHP), ammonium perchlorate-binder sandwiches and a solid propellant which utilized large unimodal AP. Sizes and construction techniques were similar to those reported by Netzer [Refs. 9 and 10], Boggs [Ref. 3] and Strahle [Ref. 5]. The specimens were mounted on end on small pedestal supports designed to fit into a test section holder. The ignition wire was stretched across the top edge of the specimen as shown in Fig. 15. Initially, the ignition electrodes were spaced too far apart. Thus, the

system was modified to bring the electrodes closer and make the ignition wire appropriately shorter. This eliminated the wire lifting off the crystal surface when electrically heated but before ignition could occur. For sandwich burners and composite propellants, a small amount of a mixture of black powder, glue and acetone was spread on the top of the wire and upper edge. This assisted in a flash ignition across the entire edge and contributed to an even regression across the width. A surveyor's transit and first surface mirror provided observation and coordination of the ignition and camera initiation sequence.

III. RESULTS AND DISCUSSION

The photographic results showed that the self-luminous interference which occurs for solid propellant combustion was eliminated by using the narrow-pass filter. In general, the results were in good agreement with previously reported results of Murphy and Netzer [Ref. 9] and Klahr and Netzer [Ref. 10]. Some significant disadvantages were identified which prevent this type optical system from also being used for detailed surface structure observations. The basic feasibility, nonetheless, of application of an optically active aperture laser schlieren system to high pressure solid propellant combustion research was demonstrated.

A schlieren photograph of the laminar portion of a city gas diffusion flame is shown in Fig. 22a. Although the quality was somewhat reduced, this schlieren record is in agreement with photographs provided by Gaydon and Wolfhard [Ref. 28]. The laminar jet at the center of the flow is clearly identifiable. The temperature and density profiles across the flame at a given height are shown qualitatively in Fig. 22c. From right to left in Fig. 22a can be seen: increasing temperature and decreasing density near the flame front (dark); density and temperature leveling off on inner side of flame (neutral); increasing density (temperature drop) approaching the center laminar jet (white); zero density gradient (inflection point) at center of laminar jet

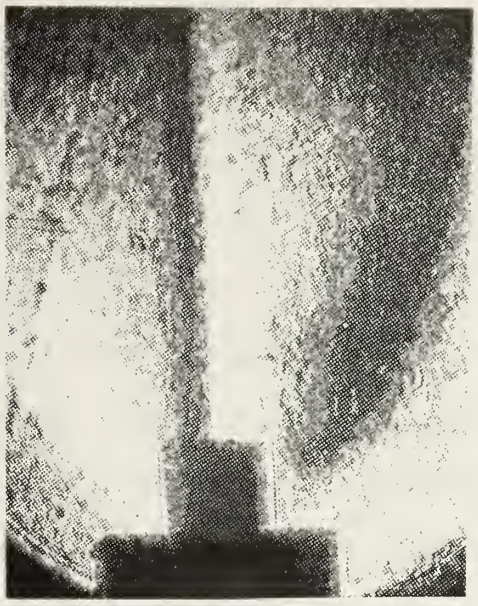

22a. City gas diffusion flame

22b. Candle flame

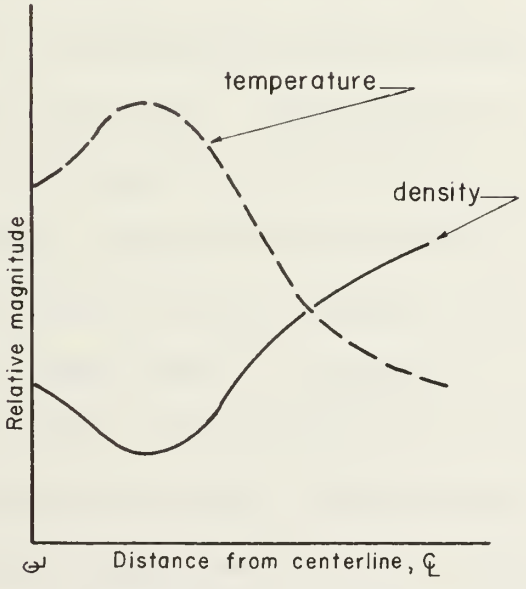

Fig 22c. Property profiles

Fig. 22 Diffusion flames

(thin neutral line); increasing temperature and decreasing density leaving the center jet (dark); temperature and density leveling off between jet and flame (neutral); increasing density (decreasing temperature) beyond the flame front (light); return to neutral background. Note the laser light diffractions along the solid boundaries of the small gas tube, along the larger solid propellant specimen support and around the curved boundary defined by the narrow-pass filter. In addition to the diffractions along solid boundaries, laser light is also extremely critical of any optical anomaly in the system. Although high quality optical members were used, several small defects were identified under laser illumination.

A schlieren photograph of a candle flame is shown in Fig. 22b. The ascending hydrocarbon vapor can be seen surrounding the wick. Again there is basic qualitative agreement with Gaydon and Wolfhard results [Ref. 28]. From right to left, the schlieren record is similar to Fig. 22a.

The still picture results for candles and gas diffusion flames were, in general, of lower quality and sensitivity than for conventional schlieren systems. There are at least three major contributing reasons: properties of the laser light itself (i.e., solid boundary diffractions, etc.), limited schlieren light-dark extremes available due to the transmission and absorption properties of the polaroid (40-70% transmission), and the limited total sensitivity, ξ,

of the reported system (16038 degrees). The latter required significant density gradients for them to be detected at all. Since these constant pressure diffusion flames were not intended as the major area of application of this schlieren system, no effort was made to match density gradients and total system sensitivity as previously discussed.

Considering solid propellants, the reduction or elimination of self-luminous interference, particularly yellow light, was a primary objective of this optical system development. Initially, results using 7277 4X reversal film indicated that the narrow-pass filter was effectively eliminating this interference from samples of AP/HTPB and AP/PBAA sandwich burners and N3 propellant (21% weight PBAN binder with 79% weight unimodal AP from 420-500μ). The final check for filtering effect on self-luminous interference was made using an AP/PBAA sandwich (binder thickness 406μ) and 7242 Ektachrome color film. The specimen was seen by direct observation to be highly self-luminous during the burn. Figure 23 shows the effective narrow-pass filter elimination of this interference.

Figure 24 shows selected frames from 7277 4X high-speed motion pictures of monopropellant ammonium perchlorate (AP) burning at various pressures. The fringing of the existing system consituted the lower resolution limit. These finely spaced fringes apparently result from interaction of the laser light with either the aperture or the lens. As measured from Fig. 24b, the resolution limit for the system,

Fig.23 AP/PBAA sandwich, 500 psi

based on fringing, was approximately 60μ. All exposure times for Fig. 24 were 80 μsec.

Fig. 24a shows a single-crystal ultra-high purity ammonium perchlorate specimen (AP-SC-UHP), 4.7mm wide, burning at 500 psi. The results were in good agreement with the color schlieren of Murphy and Netzer [Ref. 9]. Individual surface reaction sites were observed (as evidenced from the gas phase density gradients) to be distributed rather evenly across the surface. The sites appeared to be on the order of 180-280μ in width, slightly smaller than reported by Netzer [Ref. 9]. The deflagration appeared to be laminar. The definite temperature peak above the

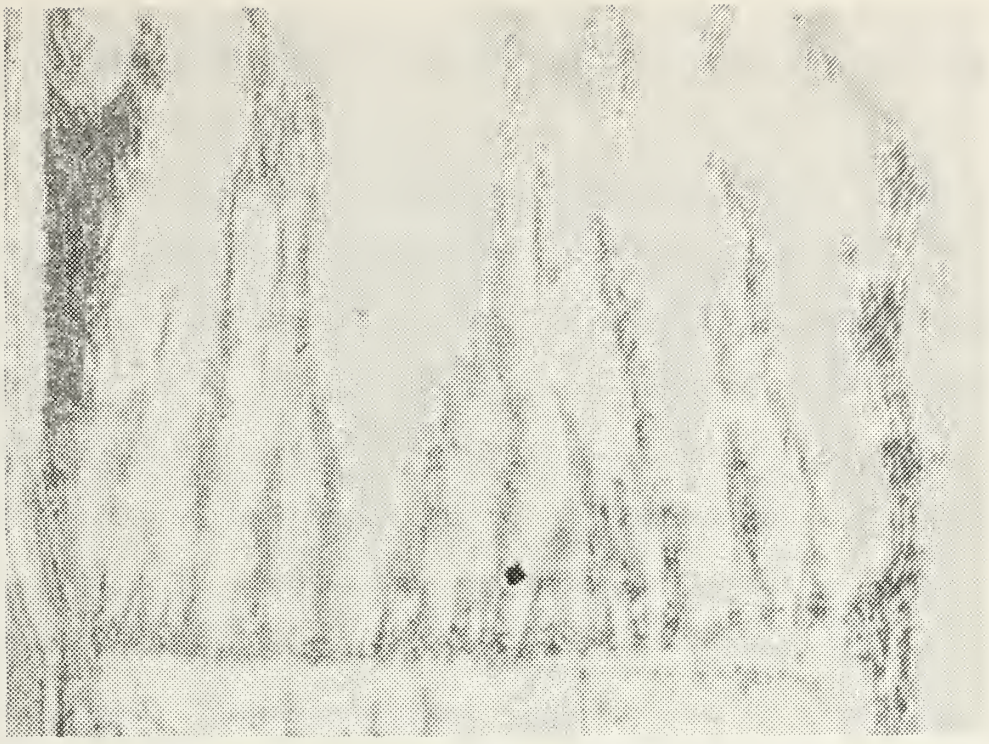

Fig.24a AP(single crystal), 500psi

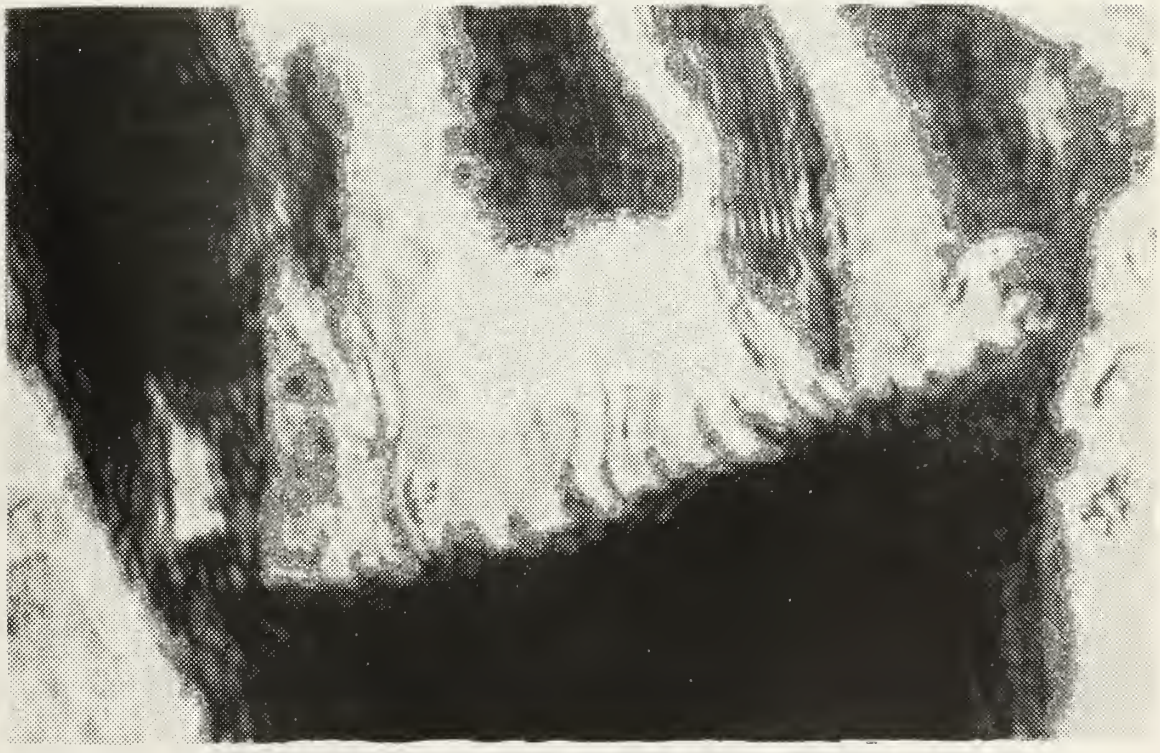

Fig 24b AP(polycrystalline), 450psi

center of the specimen, as reported by Murphy and Netzer [Ref. 9], was not observed.

Fig. 24b shows a pressed polycrystalline ammonium perchlorate specimen (PP-UHP-AP), 4.83 mm wide and 1.27 mm thick, burning at 450 psi. All (PP-UHP-AP) specimens were pressed at 30,500 psi for 20 minutes as described in Ref. 9. The light-dark schlieren shifts (evidence of individual surface reaction sites) appeared to be spaced 280-300μ across the surface with large-scale turbulence beginning about 500-600μ above the surface. The front surface of the solid phase was dark due to the fact that it was in the shadow of the laser light source and not directly illuminated. Surface definition was poor in the region of the dark schlieren gas phase-solid phase surface interface. Observable from the motion pictures was a "dancing" or apparent motion of the solid phase surface just below the burning surface. This was attributed to the reflections from the downstream bomb window. In the SC-UHP-AP specimen, this "dancing" was not observed since the transparent crystal allowed laser light transmission which overpowered any such reflections.

Smoke absorption appeared to be a major problem, particularly with the limited power laser light source. Light absorption by the smoke resulted in a darkened area, which was superimposed on any light-dark shift resulting from density gradients and confused the record interpretation.

On the right hand edge of Fig. 24b the gray region in the gas phase was thought to be smoke. Smoke accumulation was minimized by controlled purge rate.

Fig. 24c shows a PP-UHP-AP specimen, 6.1 mm wide and 1.27 mm thick, burning at 1000 psi. Fringing, light absorption by the smoke, and apparent solid phase surface motion ("dancing") were all observed. There were two major differences, however, between the 1000 psi and the 500 psi results. The first was a near-constant periodic pulsing of the burning process. At regular intervals, a very thin layer of smoke would move upward from the immediate vicinity of the surface all along the width. This smoke layer was everywhere parallel to the surface locally. That is, it reflected the instantaneous surface contour. This result was similar to those reported by Murphy and Netzer [Ref. 9]. They reported a "thermal pulsing" when their aperture was positioned to detect vertical, vice horizontal, density gradients. Boggs and Zurn [Ref. 29] similarly reported an accumulation and shedding of unreacted products on the surface of potassium-doped AP crystals, leading to a "stop and go" burning characteristic. The second difference was the lack of light-dark schlieren shifts across and just above the surface. This indicated no density gradients (i.e., approximately constant temperature) across the surface with uniform burning. Murphy and Netzer [Ref. 9] reported similar results

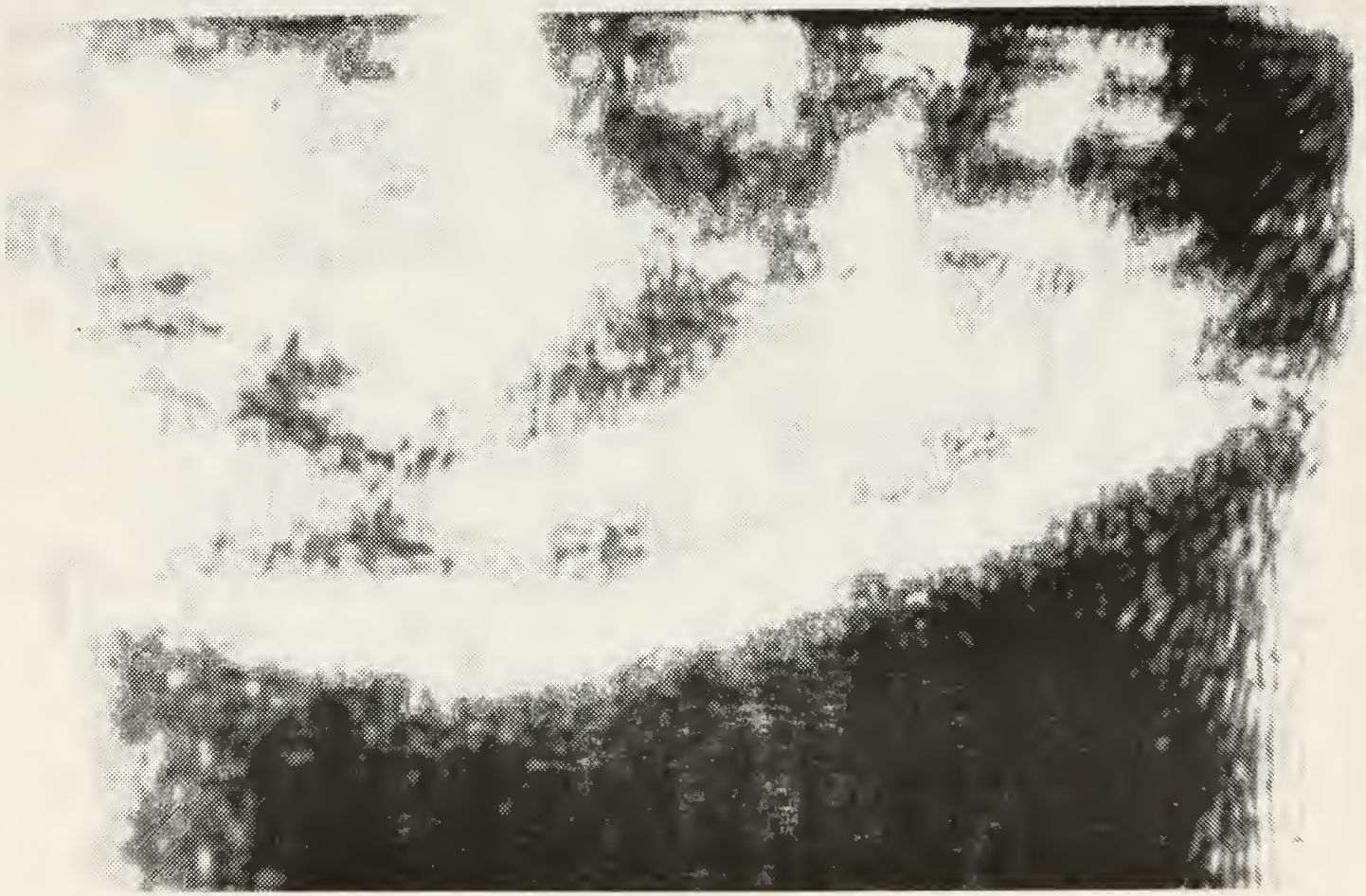

Fig.24c AP(polycrystalline), 1000psi

with "almost uniform color in the gases just above the surface."

Figure 24d shows a PP-UHP-AP specimen 6.1 mm wide and 1.27 mm thick burning at 2200 psi. The surface locally appeared to be non-uniform, with large scale turbulence very close to the surface. Density gradients were observed which extended to the burning surface. However, the smoke and fringing near the surface prevented a consistent determination of the size of the surface reaction sites. The pulsing nature observed in the 1000 psi results was not observed at 2200 psi.

Fig.24d AP(polycrystalline), 2200psi

IV. CONCLUSIONS

1. The basic feasibility of using an optically active aperture laser schlieren system for high pressure solid propellant combustion study was demonstrated.

2. The single advantage of this schlieren system over conventional schlieren systems is the self-luminous interference elimination. Self-luminous interference elimination was successfully demonstrated.

3. For applications where the self-luminous problem is nonexistent (i.e., shock pattern studies) a CW laser schlieren in general would be inferior to conventional schlieren systems. Conventional color schlieren has the added advantage over this system that schlieren effects can be more readily distinguished from variable light absorption by smoke.

4. System resolution was limited primarily by fringing. The fringing could, perhaps, be minimized or eliminated by using a bonded prism set and mirrors in place of the lenses.

5. At 500 psi, AP deflagrated in a steady manner with a rather planar surface. Individual surface reaction sites were evidenced by density gradients in the gas phase across the surface. The gas flow from the deflagrating surface was very laminar.

6. At 1000 psi, AP continued to deflagrate with a planar surface but was pulsating in nature. Surface reaction sites, if existing at all, were very small.

7. At 2200 psi, the pulsating behavior was not observed and the surface was locally non-uniform. Local reaction sites may have existed, but the gas flow immediately above the surface was very turbulent, making surface observation difficult.

8. The observations of AP deflagration using laser schlieren confirm behavior observed by other investigators who have used high speed motion pictures and post-fire examinations of quenched samples.

LIST OF REFERENCES

1. Naval Weapons Center Report NWC TP 5514, Mechanism of Combustion, by T. L. Boggs and Others, July 1973.

2. Guirao, C. and Williams, F. A., "A Model for Ammonium Perchlorate Deflagration Between 20 and 100 Atm," AIAA Journal, V. 9, No. 7, p. 1345-1356, July 1971.

3. Boggs, T. L., "Deflagration Rate, Surface Structure, and Subsurface Profile of Self-Deflagrating Single Crystals of Ammonium Perchlorate," AIAA Journal, V. 8, No. 5, May 1970.

4. Naval Weapons Center TP 4630, Deflagration of Ammonium Perchlorate, by T. L. Boggs and K. J. Kraeutle, Oct. 1968.

5. Office of Naval Research, Catalytic Behavior in Solid Propellant Combustion,by W. C. Strahle, J. C. Handley and N. Kumar, Section VI, 1 November 1973.

6. Beckstead, M. W., Derr, R. L. and Price, C. F., "A Model of Composite Solid-Propellant Combustion Based on Multiple Flames," AIAA Journal, V. 8, No. 12, p. 2200-2207, December 1970.

7. AIAA Paper No. 74-124, An Experimental Study of the Site and Mode of Action of Platonizers in Double Based Propellants, by N. Kubota and Others, February 1974.

8. Aerospace and Mechanical Sciences Report No. 1087, The Mechanism of Super-Rate Burning of Catalyzed Double Based Propellants, by N. Kubota and Others, March 1973.

9. Naval Postgraduate School Report NPS-57NT73021A, Ammonium Perchlorate and Ammonium Perchlorate-Binder Sandwich Combustion, by J. L. Murphy and D. W. Netzer, 1 February 1973.

10. Naval Postgraduate School NPS-57NT-74031, An Investigation Of Solid Propellant Combustion in Standard and High Acceleration Environments, by M. Abraham, O. A. Klahr, R. R. Gerhardt and D. W. Netzer, March 1974.

11. Picatinny Arsenal Technical Memorandum 1938, Optical Systems for Application of the Laser to Detonation Studies, by Pai-Lien Lu, August 1970.

12. Oppenheim, A. K., Urtiew, P. A., and Weinberg, F. J., "On the Use of Laser Light Sources in Schlieren-Interferometer Systems," Proceedings of the Royal Society, A, V. 291, p. 279-290, 1966.

13. Klein, M. V., Optics, p. 444-447, Wiley, 1970.

14. Boggs, T. L. and Kraeutle, K. J., "Role of the Scanning Electron Microscope in the Study of Solid Rocket Propellant Combustion; I. Ammonium Perchlorate Decomposition and Deflagration," Combustion Science and Technology, V. 1, p. 75-93, 1969.

15. Derr, R. L. and Boggs, T. L., "Role of the Scanning Electron Microscope in the Study of Solid Propellant Combustion: Part III. The Surface Structure and Profile Characteristics of Burning Composite Solid Propellants," Combustion Science and Technology, V. 1, P. 369-384, 1970.

16. Boggs, T. L. and Zurn, D. E., "The Deflagration of Ammonium Perchlorate-Polymeric Binder Sandwich Models," Combustion Science and Technology, V. 4, p. 279-292, 1972.

17. Hightower, J. D. and Price, E. W., "Experimental Studies Relating to the Combustion Mechanism of Composite Propellants," Astronautica ACTA, V. 14, p. 11-21, 1968.

18. Varney, A. M. and Strahle, W. C., "Experimental Combustion Studies of Two-Dimensional Ammonium Perchlorate-Binder Sandwiches," Combustion Science and Technology, V. 4, P. 197-208, 1972.

19. Wahlstrom, E. E., Optical Crystallography, 4th Ed., P. 370-374, Wiley, 1969.

20. Andrews, C. L., Optics of the Electromagnetic Spectrum, Ch. 19, Prentice-Hall, 1960.

21. Hartshorne, N. H. and Stuart, A., Crystals and the Polarizing Microscope, 4th Ed., P. 161-169, American Elsevier, 1970.

22. Jenkins, F. A. and White, H. E., Fundamentals of Optics, 3rd Ed., Ch. 28, McGraw-Hill, 1957.

23. Gay, P., An Introduction to Crystal Optics, Appendix D, Longmans, 1967.

24. Shubnikov, A. V., Principles of Optical Crystallography, P. 111-116, Consultants Bureau, 1960.

25. Bragg, Sir W. L. and Claringbull, G. F., The Crystalline State, V. 4, Ch. 6, Cornell University Press, 1965.

26. Robertson, J. K., Introduction to Optics: Geometrical and Physical, 4th Ed., P. 362, Van Nostrand, 1954.

27. Leipmann, H. W. and Roshko, A., Elements of GasDynamics, 8th Ed., P. 153-162, Wiley, 1957.

28. Gaydon, A. G. and Wolfhard, H. G., Flames, 3rd Ed., P. 140, Chapman and Hall, 1970.

29. T. L. Boggs and D. E. Zurn, The Deflagration of Pure and Doped Ammonium Perchlorate, Naval Weapons Center, China Lake, California, Dec. 1969.

INITIAL DISTRIBUTION LIST

		No. Copies
1.	Defense Documentation Center Cameron Station Alexandria, Virginia 22314	2
2.	Library, Code 0212 Naval Postgraduate School Monterey, California 93940	2
3.	Department Chairman, Code 57 Department of Aeronautical Engineering Naval Postgraduate School Monterey, California 93940	1
4.	Professor D. W. Netzer, Code 57NT Department of Aeronautical Engineering Naval Postgraduate School Monterey, California 93940	2
5.	LCDR James R. Andrews, USN SMC 1456 Naval Postgraduate School Monterey, California 93940	2

161483
Thesis
A527 Andrews
c.1 The development of an optically active laser Schlieren system with application to high pressure solid propellant combustion.